

# 000 001 002 003 004 005 006 007 008 009 010 011 012 013 014 015 016 017 018 019 020 021 022 023 024 025 026 027 028 029 030 031 032 033 034 035 036 037 038 039 040 041 042 043 044 045 046 047 048 049 050 051 052 053 GUMBEL DISTILLATION FOR PARALLEL DECODING OF LANGUAGE MODELS

Anonymous authors

Paper under double-blind review

## ABSTRACT

The slow, sequential nature of autoregressive (AR) language models has driven the adoption of parallel decoding methods. However, these non-autoregressive models often sacrifice generation quality because they struggle to model the complex joint distribution of token sequences. To narrow this performance gap, we introduce Gumbel Distillation, a novel distillation technique that enables parallel decoders to learn this distribution effectively. Our method leverages the Gumbel-Max trick to create a deterministic mapping from a latent Gumbel noise space to the output tokens of a high-performing AR teacher. As a model-agnostic technique, Gumbel Distillation seamlessly integrates with diverse parallel decoding architectures, including MDLM and BD3-LM. Experiments on LM1B and OpenWebText show that Gumbel Distillation substantially improves the generation quality of parallel language models, achieving a 30.0% improvement in MAUVE Score and 10.5% in generative perplexity over MDLM trained on OpenWebText dataset.

## 1 INTRODUCTION

Autoregressive (AR) language models have set the standard for text generation (Radford et al., 2019; Brown et al., 2020; Touvron et al., 2023), but their sequential, token-by-token inference process introduces significant latency, hindering their use in real-world applications. To address this bottleneck, various parallel decoding methods have emerged, including Masked Diffusion Language Models (MDLMs) (Shi et al., 2024; Sahoo et al., 2024; Arriola et al., 2025; Ou et al., 2025; Nie et al., 2025) and Multi-Token Prediction (MTP) (Cai et al., 2024; Gloeckle et al., 2024; Liu et al., 2024a). These non-autoregressive approaches accelerate inference by generating multiple tokens simultaneously. However, this speedup often comes at a cost of degradation in generation quality.

This performance gap originates from a fundamental challenge in non-autoregressive modeling (Gu et al., 2017): the difficulty of learning the complex joint probability distribution of an entire sequence. AR models elegantly handle this by factorizing the distribution into a product of conditional probabilities using the chain rule (Vaswani et al., 2017), capturing the dependency of each token on its predecessors. In contrast, to enable simultaneous prediction, parallel decoders operate under a naive assumption of conditional independence among the tokens generated in a single step. Previous works (Xiao et al., 2022; Liu et al., 2024b; Xu et al., 2024; Song & Zhou, 2025; Wu et al., 2025; Kim et al., 2025) have pointed out that the simplification, while necessary for parallelism, disrupts the natural sequential dependencies of language. For example, predicting the phrase “San Francisco” requires knowing that “Francisco” is highly dependent on the co-occurrence of “San” in the same block. When failing to capture these intricate local dependencies, parallel models can produce errors such as token repetition, resulting in text that is less coherent or grammatically flawed.

This work aims to narrow this quality gap by fundamentally improving the capacity of parallel decoders without sacrificing the speed of parallel decoding. We argue that the key is to make the learning problem for the non-autoregressive student model easier. Instead of asking it to learn the complex distribution of language from scratch, could we provide a “blueprint” from a powerful AR teacher that hints how a specific output sequence was formed?

To that end, we introduce *Gumbel Distillation*, a novel distillation framework that enables a non-autoregressive student to learn the complex token dependencies captured by an AR teacher. The core of our method is the Gumbel-Max trick, which we use to establish a deterministic mapping from a simple Gumbel noise distribution to the target output sequence from the AR teacher. The resulting noise vector serves as the latent “blueprint” to its paired token sequence, uniquely encoding the

054 sampling decisions made by the teacher. By training the student to reconstruct the text conditioned  
 055 on the Gumbel noise, we turn the difficult joint-distribution matching problem into a supervised  
 056 learning problem.

057 A key advantage of our approach is its simplicity and general applicability. Because the distillation  
 058 process is framed as adding a conditional input, Gumbel Distillation can be seamlessly integrated as  
 059 a plug-and-play module into a wide variety of existing parallel decoding architectures. It does not  
 060 require complex changes to the model’s structure, making it a flexible tool for enhancing different  
 061 frameworks. We demonstrate this by applying Gumbel Distillation to state-of-the-art architectures,  
 062 including MDLM (Sahoo et al., 2024), BD3-LM (Arriola et al., 2025) and Medusa (Cai et al., 2024),  
 063 showing it serves as a simple yet powerful complement. Our experiments validate that Gumbel  
 064 Distillation significantly improves generation quality, enabling high-quality multi-token decoding.

065 Our main contributions are as follows:

- 067 • We propose Gumbel Distillation, a novel framework for distilling knowledge from an AR  
 068 teacher into a parallel student. The method enables the student to model the joint token  
 069 distribution by learning a direct mapping from Gumbel noise to the teacher’s output.
- 070 • To demonstrate the simplicity and effectiveness of our approach, we integrate it with state-  
 071 of-the-art parallel decoding frameworks, including MDLM, BD3-LM and Medusa, improv-  
 072 ing their performance while making minimal architectural changes.
- 073 • Our extensive experiments validate that our method successfully alleviates the gap between  
 074 autoregressive quality and parallel decoding efficiency, achieving state-of-the-art results in  
 075 high-quality, accelerated text generation with parallel decoding.

## 077 2 RELATED WORK

079 **Diffusion Language Models** Inspired by the success of diffusion models in visual domains (Ho  
 080 et al., 2020; Song et al., 2021; Liu et al., 2022; Lipman et al., 2022), a number of works have  
 081 explored diffusion language models (dLLMs) by extending the technique to text domains. An in-  
 082 tuitive approach is to model text in a continuous space and apply diffusion directly (Li et al., 2022;  
 083 Gong et al., 2023; Han et al., 2022; Dieleman et al., 2022). To fit the discrete nature of text, an-  
 084 other approach focuses on using discrete processes featuring forward and reverse dynamics, with  
 085 the foundational work laid out by D3PM (Austin et al., 2021). Numerous variants follow (Hooge-  
 086 boom et al., 2021; He et al., 2022; Campbell et al., 2022; Sun et al., 2022; Chen et al., 2022; Wu  
 087 et al., 2023; Zheng et al., 2023; Gat et al., 2024), with masked diffusion language models being a  
 088 specific focus for recent research (Chen et al., 2024; Shi et al., 2024; Nie et al., 2024; Zheng et al.,  
 089 2024; Lou et al., 2024; Ou et al., 2025; von Rütte et al., 2025; Kim et al., 2025) due to their strong  
 090 performance. Notably, MDLM (Sahoo et al., 2024) derived a simplified objective for masked diffu-  
 091 sion that connects the operation of unmasking tokens to a true generative process. BD3-LM (Arriola  
 092 et al., 2025) builds upon MDLM to introduce a hybrid approach that models sequences in a block-  
 093 wise manner while applying diffusion within each block, enabling flexible length generation and  
 094 improved inference efficiency through kv-caching. In our paper, we apply Gumbel Distillation to  
 095 these two architectures as examples to show the effectiveness and flexibility of our method.

096 Encouraged by the above works, recent efforts have scaled diffusion language models to billions  
 097 of parameters (Nie et al., 2025; Gong et al., 2025; Ye et al., 2025). Furthermore, commercial suc-  
 098 cess like Seed Diffusion (Song et al., 2025), Mercury Coder (Labs et al., 2025) and Gemini Dif-  
 099 fusion (DeepMind, 2025) have also demonstrated their practical viability, achieving performance  
 100 comparable to state-of-the-art AR models with significantly faster speed of inference.

101 **Multi-Token-Prediction** Multi-token-prediction (MTP) strategies (Cai et al., 2024; Gloeckle  
 102 et al., 2024; Liu et al., 2024a; Samragh et al., 2025) enable faster, flexible sampling of AR lan-  
 103 guage models. However, current MTP models often predict the probability of each token in a block  
 104 independently, which is an issue also relevant to diffusion language models. Song & Zhou (2025);  
 105 Zhu et al. (2025) argues that this naive conditional independence assumption greatly limits the ca-  
 106 pacity of the model distribution. Although the issue can be alleviated via corrections to the inference  
 107 procedure (Gu et al., 2017; Leviathan et al., 2023; Santilli et al., 2023; Shi et al., 2024) such as spec-  
 108 ulative decoding. Our Gumbel Distillation method points to a fundamental solution that in principle  
 109 allows the model to train and infer from the true joint distribution.

108 **Knowledge Distillation for Parallel Decoding** A key application of knowledge distillation is to  
 109 accelerate inference by training a parallel student model to mimic a powerful AR teacher. This  
 110 line of research was pioneered by Gu et al. (2017), which introduced sequence-level knowledge  
 111 distillation to train a parallel student on the outputs of an AR teacher. This foundational technique  
 112 spurred the development of parallel models for machine translation (Ghazvininejad et al., 2019;  
 113 Gu et al., 2019; Kasai et al., 2021). More recently, some approaches (Gu et al., 2023; Kou et al.,  
 114 2024) have adapted these principles for general language models. Different from these works, our  
 115 proposed Gumbel Distillation distills from the AR teacher’s internal sampling process, which allows  
 116 the parallel student to learn the full probability landscape.

### 117 3 BACKGROUND

119 **The Challenge of Parallel Decoding** An AR language model, denoted as  $p^*$ , generates a se-  
 120 quence of tokens  $\mathbf{x}^{1:n} = (x^1, \dots, x^n)$  one at a time.<sup>1</sup> The probability of the sequence is factorized  
 121 as  $p^*(\mathbf{x}^{1:n}) = \prod_{i=1}^n p^*(x^i | \mathbf{x}^{<i})$ , where  $\mathbf{x}^{<i}$  represents the preceding tokens. This sequential fac-  
 122 torization effectively captures the dependencies between tokens, leading to high-quality output, but  
 123 at the cost of slow, iterative inference.

124 In contrast, *parallel decoding* methods accelerate this process by generating multiple tokens at once.  
 125 Instead of a single token  $x^i$ , these models predict a *subset* of all tokens, denoted by  $\mathbf{x}^{\mathcal{I}}$ , where  $\mathcal{I}$  is a  
 126 set of token indices. The already generated tokens  $\mathbf{x}^{-\mathcal{I}}$ , serve as the context. This paradigm applies  
 127 to various parallel decoding architectures; for instance, in MTP (Cai et al., 2024; Gloeckle et al.,  
 128 2024; Liu et al., 2024a),  $\mathcal{I}$  is the set of indices for a block of future tokens, and in MDLMs (Shi  
 129 et al., 2024; Sahoo et al., 2024; Arriola et al., 2025; Ou et al., 2025; Nie et al., 2025),  $\mathcal{I}$  is the set of  
 130 indices for the tokens to unmask. However, to enable simultaneous prediction for all indices in  $\mathcal{I}$ ,  
 131 these models are often forced to adopt a conditional independence assumption. They approximate  
 132 the true, sequentially dependent distribution of the AR model  $p^*$  with a block-wise factorized one:

$$p_{\theta}(\mathbf{x}^{\mathcal{I}} | \mathbf{x}^{-\mathcal{I}}) = \prod_{i \in \mathcal{I}} p_{\theta}(x^i | \mathbf{x}^{-\mathcal{I}}).$$

135 This assumption ignores the dependencies within the target set  $\mathbf{x}^{\mathcal{I}}$ , and as a result, these architectures  
 136 fail to capture the local structure essential for natural language. **We aim to mitigate the quality**  
 137 **degradation caused by this factorization.**

138 **Gumbel-Max Trick** The Gumbel-Max trick (Gumbel, 1954) is a reparameterization technique for  
 139 sampling from a categorical distribution. To sample from a category  $X \in \{1, \dots, V\}$  defined by  
 140 the Boltzmann distribution with a vector of logits  $\mathbf{l} = (l_1, \dots, l_V) \in \mathbb{R}^V$ :

$$P(X = k) = \exp(l_k) / \sum_{j=1}^V \exp(l_j),$$

144 we can first draw i.i.d. standard Gumbel noise  $\{\xi_k \sim \mathcal{G}(0, 1)\}_{k=1}^V$ , and then compute:

$$Y = \arg \max_k (l_k + \xi_k).$$

147 The resulting sample  $Y$  has the exact *same* distribution as  $X$ . In practice, a common method to  
 148 sample  $\xi \sim \mathcal{G}(0, 1)$  is via inverse transform sampling, where we first sample a Uniform variable  
 149  $u \sim \mathcal{U}[0, 1]$ , and then calculate the Gumbel noise as  $\xi = -\log(-\log u)$ .

150 One crucial insight here is that we can reframe the sampling process: the randomness is externalized  
 151 into the Gumbel noise vector  $\xi = (\xi_1, \dots, \xi_V) \in \mathbb{R}^V$ . While categorical sampling is stochastic, the  
 152 argmax function in Gumbel-Max is fully *deterministic* once the logits and the noise are known.

### 153 4 METHOD

155 Our primary objective is to design a parallel decoder,  $p_{\theta}$ , such that its output can match the high-  
 156 quality output of a powerful AR teacher,  $p^*$ . Formally, given an AR teacher model:

$$p^*(\mathbf{x}^{1:n}) = \prod_{i=1}^n p^*(x^i | \mathbf{x}^{<i}), \quad \text{where } \forall i, p^*(x^i = k | \mathbf{x}^{<i}) = \frac{\exp(f^*(\mathbf{x}^{<i})_k)}{\sum_{j=1}^V \exp(f^*(\mathbf{x}^{<i})_j)},$$

160 where  $f^*(\cdot)_k$  denotes the  $k$ -th logit predicted by the teacher, we aim to solve the following problem:

161 <sup>1</sup>Throughout the paper, we use bold symbols for vectors.

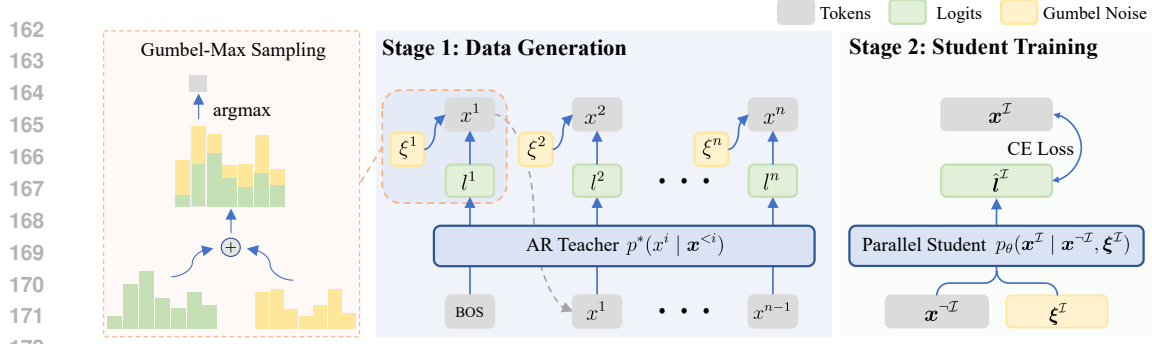


Figure 1: **A conceptual overview of Gumbel Distillation.** The distillation process consists of two steps: (1) **Data Generation:** An autoregressive teacher model’s sampling process is combined with Gumbel noise to deterministically generate pairs of token sequences and their corresponding Gumbel noise. In practice, one could alternatively extract  $\{\xi\}$  in parallel based on an offline training corpus (Section 4.1); (2) **Student Training:** A parallel student model is trained to predict a target subset of tokens, conditioned on both the context and the Gumbel noise from the teacher.

*How can we train a parallel decoder  $p_\theta$  to generate a subset of tokens  $\mathbf{x}^T$  simultaneously, while ensuring its output distribution  $p_\theta(\mathbf{x}^T | \mathbf{x}^{-T})$  matches the teacher’s distribution  $p^*(\mathbf{x}^T | \mathbf{x}^{-T})$ ?*

However, this objective is notoriously difficult. A naive approach of using a neural network to directly model the conditional distribution  $p_\theta(\mathbf{x}^T | \mathbf{x}^{-T})$  can easily become intractable. This is because the model would need to output a probability distribution over a discrete space of size  $V^{|\mathcal{I}|}$ , which grows exponentially with the number of tokens  $|\mathcal{I}|$  generated in parallel.

To overcome these challenges, our key insight is to reframe the difficult distribution matching problem into a more manageable **supervised learning problem**. We achieve this by reformulating the teacher’s stochastic sampling process as a fixed function of random noise. At each generation step, the AR model samples a token from a categorical distribution. The Gumbel-Max trick provides an equivalent formulation: adding random Gumbel noise to the logits and taking the argmax. This reveals a crucial link: for any sequence  $\mathbf{x}^{1:n}$  generated by the teacher, there exists a corresponding sequence of Gumbel noise  $\xi^{1:n}$  that produces it, thereby creating an explicit mapping from noise to text. Consequently, instead of directly learning the joint distribution over a block of multiple tokens, the student’s task is simplified to learning this deterministic function:  $p_\theta(\mathbf{x}^T | \mathbf{x}^{-T}, \xi^T)$ .

#### 4.1 GUMBEL DISTILLATION: FRAMEWORK

Building on the above intuition, we detail Gumbel Distillation as a two-stage framework (Figure 1). The process begins with data generation to produce training instances from the teacher, followed by student training, where the parallel decoder learns the noise-conditioned mapping.

**Stage 1: Data Generation** In the first stage, we use the AR teacher  $p^*$  to generate a complete pair consisting of a full token sequence  $\mathbf{x}^{1:n}$  and its corresponding Gumbel noise sequence  $\xi^{1:n}$ . This initial step is inherently sequential. From this complete pair, we then construct a training example for our parallel student based on its architecture. By selecting a subset of indices  $\mathcal{I} \subseteq \{1, \dots, n\}$  to be the prediction target, we partition the data into triplets  $(\mathbf{x}^{-\mathcal{I}}, \xi^{\mathcal{I}}, \mathbf{x}^{\mathcal{I}})$ , where:

- $\mathbf{x}^{-\mathcal{I}}$  is the context, consisting of the tokens not in our target set.
- $\xi^{\mathcal{I}}$  is the conditional Gumbel noise for the target positions.
- $\mathbf{x}^{\mathcal{I}}$  is the target token subset that the student learns to predict.

**Stage 2: Student Training** Once the training data is prepared, the second stage involves training a parallel student decoder  $p_\theta$  (e.g. masked diffusion model or multi-token-prediction model) to predict the target token subset  $\mathbf{x}^{\mathcal{I}}$  simultaneously. The student model is conditioned on both the context  $\mathbf{x}^{-\mathcal{I}}$  and the corresponding Gumbel noise for the target positions  $\xi^{\mathcal{I}}$ , and the training objective is to maximize the conditional log-likelihood:

$$\mathcal{L} = -\mathbb{E}_{(\mathbf{x}^{-\mathcal{I}}, \xi^{\mathcal{I}}, \mathbf{x}^{\mathcal{I}}) \sim \text{data}} [\log p_\theta(\mathbf{x}^{\mathcal{I}} | \mathbf{x}^{-\mathcal{I}}, \xi^{\mathcal{I}})].$$

One crucial implementation detail in this framework is how we obtain the set of distillation targets  $(\xi^{1:n}, \mathbf{x}^{1:n})$  from the AR teacher. We propose two practical methods for this extraction process. The

---

216 **Algorithm 1** Parallel Gumbel Sampling for a Sequence

---

217 **Require:** Ground-truth token sequence  $x^{1:n} = (x^1, \dots, x^n)$

218 **Require:** Sequence of logit vectors  $l^{1:n} = (l^1, \dots, l^n)$ , where each  $l^i \in \mathbb{R}^V$

219 **Ensure:** Posterior Gumbel sample sequence  $\xi^{1:n} = (\xi^1, \dots, \xi^n)$ , where each  $\xi^i \in \mathbb{R}^V$

220 1: **for all**  $i \in \{1, \dots, n\}$  **in parallel do**

221 2:    $p_{x^i} \leftarrow \text{Softmax}(l^i)_{x^i}$  ▷ Result is a scalar probability

222 3:   Sample auxiliary noises:  $\zeta_0 \sim \mathcal{G}(0, 1)$  and  $\zeta \in \mathbb{R}^V \sim \mathcal{G}(0, 1)^V$

223 4:    $\xi^i \leftarrow -\log(\exp(-\zeta) + p_{x^i} \exp(-\zeta_0))$  ▷ Assigns to the full vector  $\xi^i$

224 5:    $\xi_{x^i}^i \leftarrow \zeta_0 - \log p_{x^i}$  ▷ Overwrites a single scalar component of  $\xi^i$

225 6: **end for**

226 7: **return**  $\xi^{1:n}$

---

227

228

229 first arises naturally from the Gumbel-Max procedure, while the second approximately equivalent

230 method offers significant computational advantages by allowing us to parallelize the computation.

231 **Sequential Gumbel Extraction** The most straightforward approach is to perform sequential sam-  
232 pling from the teacher model  $p^*$ . For each position  $i = 1, \dots, n$ , we first draw a Gumbel noise  
233 vector  $\xi^i \in \mathbb{R}^V$  and then recursively apply the Gumbel-Max trick to generate the next token  $x^i$ ,

234

$$235 x^i = \arg \max_k (\xi_k^i + f^*(x^{<i})_k), \text{ where } \xi_k^i = -\log(-\log(u_k^i)), u_k^i \sim \text{Uniform}(0, 1).$$

236

237 By repeating this autoregressive process for the entire sequence, we can generate pairs of full se-  
238 quences  $(\xi^{1:n}, x^{1:n})$ , and the mapping from the noise  $\xi^{1:n}$  to the text  $x^{1:n}$  is deterministic given that  
239 the AR model is fixed and deterministic. While computationally intensive, this approach allows us  
240 to generate an unlimited amount of high-fidelity distillation data, which can then be partitioned into  
241 training triplets as described above.

242 **Parallel Gumbel Extraction** While the sequential strategy is simple and robust, it requires many  
243 forward passes through the teacher model to generate data. As a highly efficient alternative, we can  
244 leverage an existing text corpus by assuming its data was drawn from the teacher’s distribution  $p^*$ .  
245 Given a token sequence  $x^{1:n}$  from the corpus, we first perform a single forward pass with the teacher  
246 model to get the corresponding logits  $l^{1:n}$ . The problem is then reframed as recovering the posterior  
247 distribution of the Gumbel noise  $P(\xi^{1:n}|x^{1:n}, l^{1:n})$  that would reconstruct the original text.

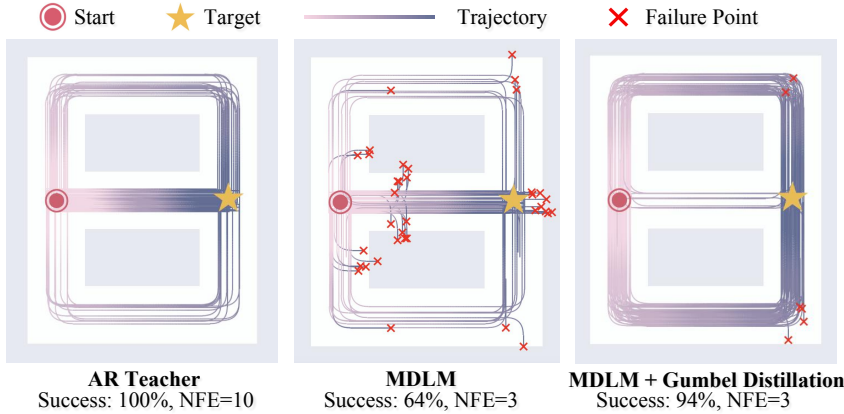
248 To this end, the following theorem provides a direct, analytical method for sampling from this pos-  
249 terior, enabling us to extract Gumbel noise for an entire sequence in parallel. Using Algorithm 1,  
250 we can sample the Gumbel noise vectors for every token in a sequence via one single forward pass  
251 through the teacher model, which significantly accelerates the data generation process. A detailed  
252 version of the theorem and its proof is available in Appendix B

253 **Theorem 4.1** (Gumbel-Max Posterior Sampling). *Assume token  $x$  is drawn from the softmax distri-  
254 bution of a logits vector  $l = (l_1, \dots, l_V)$ , using the Gumbel-Max trick with a Gumbel noise vector  
255  $\xi = (\xi_1, \dots, \xi_V)$ , i.e.  $x = \arg \max_k (l_k + \xi_k)$ . A valid sample  $\xi$  from the posterior distribu-  
256 tion  $p(\xi|X = x)$  that satisfies the constraint can be drawn by the procedure which we extend for  
257 sequences in Algorithm 1.*

258 4.2 GUMBEL DISTILLATION: APPLICATION

259 Our framework benefits from its simplicity and generality. By reformulating the learning problem  
260 as a supervised task conditioned on Gumbel noise, Gumbel Distillation can serve as a versatile,  
261 plug-and-play enhancement for existing parallel decoders. In this section, we show how Gumbel  
262 Distillation can be seamlessly integrated into two popular families of such models: Masked Diffu-  
263 sion Language Models and Multi-Token-Prediction Models.

264 **Conditioning Masked Diffusion Language Models** Masked Diffusion Language Models (e.g.,  
265 MDLM (Sahoo et al., 2024), BD3-LM (Arriola et al., 2025)) operate by training a model to recover  
266 the original text from a corrupted version, where masking is used for the corruption process. In our  
267 setup, given a text sequence where a subset of tokens  $x^{\mathcal{I}}$  has been replaced by `[MASK]`, the model  
268 learns to predict the original tokens  $x^{\mathcal{I}}$  based on the unmasked context  $x^{-\mathcal{I}}$ . To apply Gumbel  
269 Distillation, we simply augment the model’s input. Instead of predicting the masked tokens from the



284 **Figure 2: A toy maze problem illustrating how Gumbel Distillation helps a student model learn**  
285 **a structured task.** The goal is to generate a valid path from a start (`<bos>`) to a target (`<eos>`)  
286 using a simple vocabulary (up, down, left, right). The figure visualizes 100 generated paths  
287 from each model, slightly jittered for visualization. The baseline MDLM frequently fails, produc-  
288 ing incoherent paths, indicating its difficulty in modeling the joint distribution of the sequence. In  
289 contrast, our Gumbel-conditioned model successfully finds valid paths, closely matching the per-  
290 formance of the AR teacher but at a fraction of the generation cost (NFE = 3 steps vs. 10 steps).

291 context alone, the student model  $p_\theta$  is now also conditioned on the Gumbel noise  $\xi^{\mathcal{I}}$  corresponding  
292 to the target tokens. The learning objective becomes maximizing  $p_\theta(\mathbf{x}^{\mathcal{I}} | \mathbf{x}^{-\mathcal{I}}, \xi^{\mathcal{I}})$ .

293 A crucial design choice is how to inject the Gumbel signal. We found it most effective to process the  
294 Gumbel noise for the masked tokens,  $\xi^{\mathcal{I}}$ , into a vector on the model’s vocabulary embedding space  
295 via a softmax normalization followed by a learned linear projection. Softmax function constrains the  
296 Gumbel values to  $(0, 1)$ , controlling for its large tails, while preserving the relative ranks in Gumbel  
297 that encode the teacher’s sampling choice. These processed Gumbel embeddings then replace the  
298 standard `[MASK]` token embeddings in the input sequence. In this way, the uninformative `[MASK]`  
299 tokens are substituted with a rich “blueprint” from the teacher, guiding the student for prediction.  
300 Full implementation details can be found in Appendix C.1.

301 The visualization in Figure 2 provides a compelling toy example of this process, where we apply  
302 Gumbel Distillation to MDLM on a simple maze navigation task by defining the valid action se-  
303 quence as the language. The Gumbel-conditioned MDLM improves greatly over the baseline to  
304 match the AR teacher’s performance with a much lower NFE.

305 **Conditioning Multi-Token-Prediction Models** Multi-Token Prediction (MTP) models, such as  
306 Medusa (Cai et al., 2024), accelerate decoding by using multiple “heads” to simultaneously generate  
307 a block of future tokens. At a given generation step  $i$  with  $k$  heads, this block corresponds to the  
308 target indices  $\mathcal{I} = \{i + 1, \dots, i + k\}$ . To apply Gumbel Distillation, we train these heads to predict  
309 the target block  $\mathbf{x}^{\mathcal{I}}$  conditioned on the preceding context  $\mathbf{x}^{-\mathcal{I}}$  and the corresponding Gumbel noise  
310 blueprint  $\xi^{\mathcal{I}}$  from the teacher.

311 The Gumbel noise is processed into a conditioning vector and provided to each prediction head.  
312 This gives the heads direct guidance on the joint distribution of the token sequence, helping them  
313 overcome the standard conditional independence assumption and propose more coherent candidate  
314 blocks for verification. Full implementation details can be found in Appendix C.2.

## 315 5 EXPERIMENTS

317 In this section, we empirically validate Gumbel Distillation. We demonstrate its effectiveness and  
318 generality on Masked Diffusion Models (Section 5.1) and Multi-Token Prediction Models (Section  
319 5.2). We conclude with ablation studies (Section 5.3) to justify our method’s design.

### 320 5.1 GUMBEL DISTILLATION FOR MASKED DIFFUSION MODELS

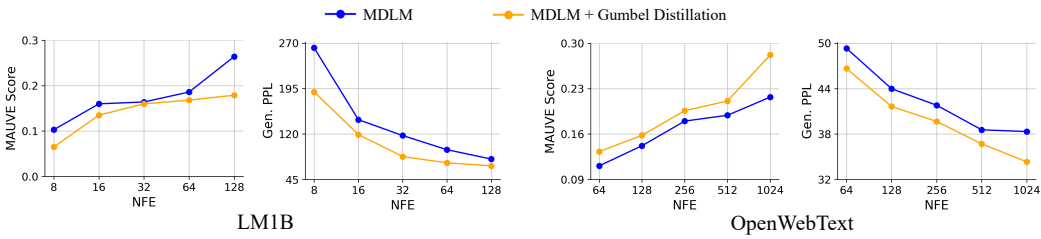
322 **Experimental Setup** To evaluate Gumbel Distillation, we integrate it into two state-of-the-art  
323 masked diffusion frameworks. **MDLM** and **BD3-LM**. The autoregressive teacher model for all  
distillation experiments is **GPT-2-Large**. For our main results, we use the efficient parallel gumbel

324  
 325 **Table 1: Main results for unconditional text generation.** Our method consistently outperforms  
 326 all baselines on both MAUVE and Generative Perplexity (Gen. PPL). Models were trained for 1M  
 327 steps on LM1B (length 128) and OpenWebText (length 1024). Best non-AR scores are in bold.

|   | LM1B                      |                          | OpenWebText               |                          |
|---|---------------------------|--------------------------|---------------------------|--------------------------|
|   | MAUVE Score( $\uparrow$ ) | Gen. PPL( $\downarrow$ ) | MAUVE Score( $\uparrow$ ) | Gen. PPL( $\downarrow$ ) |
| AR  | 0.465                     | 36.42                    | 0.691                     | 14.10                    |
| MDLM                                      | 0.179                     | 78.74                    | 0.217                     | 38.34                    |
| MDLM + Gumbel Distillation                | <b>0.264</b>              | <b>67.64</b>             | <b>0.282</b>              | <b>34.33</b>             |
| BD3-LM ( $L' = 4$ )                       | 0.193                     | 56.98                    | 0.251                     | 26.40                    |
| BD3-LM ( $L' = 4$ ) + Gumbel Distillation | <b>0.291</b>              | <b>46.06</b>             | <b>0.304</b>              | <b>24.37</b>             |

334  
 335 **Table 2: Qualitative evaluation using Gemini-2.5-pro as an LLM judge on OpenWebText.**  
 336 Scores are on a 1-10 scale (higher is better). Gumbel Distillation shows clear improvements across  
 337 most dimensions, with the most significant and consistent gains observed in **Clarity** and **Factuality**.

| Model                        | Clarity              | Grammaticality       | Factuality           | Style                | Creativity          |
|------------------------------|----------------------|----------------------|----------------------|----------------------|---------------------|
| MDLM                         | 2.44                 | 2.22                 | 2.70                 | 2.32                 | 2.22                |
| MDLM + Gumbel Distillation   | <b>2.86</b> (+17.2%) | <b>2.57</b> (+15.8%) | <b>3.31</b> (+22.6%) | <b>2.57</b> (+10.8%) | <b>2.36</b> (+6.3%) |
| BD3-LM                       | 2.89                 | 2.95                 | 3.21                 | 3.34                 | <b>2.75</b>         |
| BD3-LM + Gumbel Distillation | <b>3.41</b> (+18.0%) | <b>3.22</b> (+9.2%)  | <b>3.78</b> (+17.7%) | <b>3.35</b> (+0.2%)  | 2.68 (-2.5%)        |



352 **Figure 3: Generative Perplexity and MAUVE Score vs. Number of Function Evaluations (NFE)**  
 353 **on LM1B and OpenWebText.** Our method (Gumbel Distillation) consistently outperforms the  
 354 baselines, achieving lower perplexity for a given number of evaluations.

355 extraction method (detailed in Section 4.1) to generate the distillation data in an online manner  
 356 while iterating through the existing dataset. We compare our method against two baselines: (1) an  
 357 **AR model** with the same size as the students for a fair quality comparison; (2) the **student models**  
 358 **trained from scratch** (MDLM and BD3-LM) on raw text without distillation, which establishes the  
 359 performance of the base parallel architectures. Full implementation details are in Appendix C.1.

360  
 361 **Results on Unconditional Text Generation** We evaluate performance using two key metrics.  
 362 Generative Perplexity (Gen. PPL) measures token-level fluency. For a more holistic assessment of  
 363 quality and diversity, we use the MAUVE score (Liu et al., 2021), which compares the generated  
 364 text distribution to a human reference. As shown in Table 1, our method, Gumbel Distillation,  
 365 consistently and significantly improves the performance of the baseline models in unconditional text  
 366 generation. For instance, when applied to MDLM on OpenWebText, Gumbel Distillation reduces  
 367 generative perplexity by 10.5% and boosts the MAUVE score by 30.0%. These substantial gains are  
 368 consistent across other results on BD3-LM, demonstrating our approach’s general effectiveness.

369  
 370 **LLM-based Evaluation** To complement our statistical metrics with a qualitative assessment, we  
 371 used Gemini-2.5-pro (Comanici et al., 2025) to score the text samples generated by models trained  
 372 on OWT. As shown in Table 2, we use Gemini-2.5-pro to judge all models on five dimensions:  
 373 clarity, grammaticality, factuality, style, and creativity. Full details on the evaluation prompt and  
 374 setup can be found in Appendix D.3. The results are consistent with our earlier findings using  
 375 Gen. PPL and MAUVE score, confirming that Gumbel Distillation leads to a clear improvement  
 376 in perceived generation quality. For both MDLM and BD3-LM, we see consistent gains across all  
 377 dimensions, with particularly strong improvements in Factuality and Clarity. This suggests that the  
 378 Gumbel conditioning helps the student model generate more coherent and grounded text.

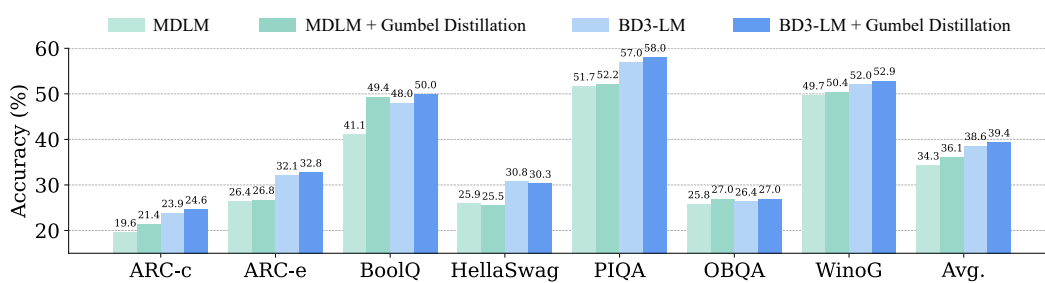


Figure 4: **Zero-shot performance on common-sense reasoning and question answering benchmarks.** Our Gumbel Distillation consistently improves accuracy over the baseline models across a suite of eight tasks. All scores are percentages (%).

**Performance vs. Number of Sampling Steps** In Figure 3, we plot MAUVE score and generative perplexity against the number of inference steps (NFE), using the efficient ancestral sampler from Sahoo et al. (2024) for all models. The results show two key advantages. First, at any given NFE, our models achieve a stronger perplexity than the baselines. Second, our models reach a high level of quality in far fewer steps compared to the baseline models. This efficiency gain suggests that the Gumbel “blueprint” provides a more direct signal, enabling the student model to converge on a high-quality output during the iterative generation process.

**Zero-shot Benchmark Performance** We evaluate the language understanding capabilities of the models trained on OWT on a wide range of question answering tasks. Following von Rütte et al. (2025), our selected benchmarks include ARC-e and ARC-c (Clark et al., 2018), BoolQ (Clark et al., 2019), HellaSwag (Zellers et al., 2019), PIQA (Bisk et al., 2020), OpenBookQA (Mihaylov et al., 2018) and Winogrande (Sakaguchi et al., 2021). The results, presented in Figure 4, show that Gumbel Distillation effectively transfers the reasoning capabilities of the AR teacher to the parallel student models. For instance, applying our method to MDLM improves its average accuracy across all benchmarks from 34.3% to 36.1%. We observe consistent gains across the board, with a particularly notable improvement in BoolQ. Similar improvements are seen when applying our method to BD3-LM (from 38.6% to 39.4%), demonstrating the robustness of our approach. This demonstrates that the student not only mimics the teacher’s fluency but also inherits its knowledge and common-sense reasoning abilities, substantially improving the performance on these challenging tasks.

## 5.2 GUMBEL DISTILLATION FOR MULTI-TOKEN PREDICTION

We apply Gumbel Distillation to a MTP framework based on Medusa (Cai et al., 2024). This setup provides a direct, single-step test of a model’s ability to capture the joint distribution of a sequence.

**Experimental Setup** We follow the Medusa-1 setup, using a frozen GPT-2-Small as the backbone model and training four parallel MTP heads. The heads are trained on the OpenWebText dataset using our Gumbel distillation method, with the backbone itself serving as the teacher in a self-distillation setup. We use typical acceptance for speculative decoding, and measure the conditional acceptance rate for each head. A token proposed by a later head is only verified if all preceding tokens in the block have already been accepted. This metric is a strong indicator of the coherence of the entire predicted sequence. Full implementation details are in Appendix C.2.

**Results and Analysis** The results in Table 3 show that Gumbel conditioning significantly improves the performance of the MTP heads. Our method boosts the acceptance rate across all positions and increases the average number of accepted tokens per step. Crucially, the performance gains become progressively larger for later heads, increasing from a +4.5% improvement for the first prediction head to a +22.0% gain for the final head. This trend provides strong evidence that Gumbel Distillation helps the MTP heads learn the stronger sequential dependencies required to predict tokens further into the future, directly addressing the core challenge of modeling a joint distribution.

Table 3: **Per-position acceptance rates of MTP heads trained on top of a frozen GPT-2 backbone.** The improvement grows for later positions, showing the effectiveness of Gumbel Distillation in modeling stronger sequential dependencies.

|                 | Baseline | + Gumbel       |
|-----------------|----------|----------------|
| Head 0 (NTP)    | 0.987    | 0.990 (+0.3%)  |
| Head 1          | 0.445    | 0.465 (+4.5%)  |
| Head 2          | 0.310    | 0.344 (+11.0%) |
| Head 3          | 0.264    | 0.322 (+22.0%) |
| Accepted Length | 1.609    | 1.691          |

432 Table 4: **Consolidated ablation study using MDLM on LM1B.** Parallel Gumbel Extraction is  
 433 superior to the sequential method. The specific Gumbel distribution is critical, as replacing it with  
 434 Gaussian noise degrades performance, and Uniform noise leads to mode collapse.

| 436 | Parallel<br>Gumbel Extraction | Sequential<br>Gumbel Extraction | Gumbel<br>Noise | Gaussian<br>Noise | Uniform<br>Noise | MAUVE Score(↑) | Gen. PPL (↓) |
|-----|-------------------------------|---------------------------------|-----------------|-------------------|------------------|----------------|--------------|
| 437 | ✓                             |                                 | ✓               |                   |                  | <b>0.264</b>   | <b>67.64</b> |
| 438 |                               | ✓                               | ✓               |                   |                  | 0.189          | 86.38        |
| 439 | ✓                             |                                 |                 | ✓                 |                  | 0.242          | 81.43        |
| 440 |                               |                                 |                 |                   | ✓                | 0.097          | -            |

### 441 5.3 ABLATION STUDIES

442 **Impact of Sequential vs. Parallel Gumbel Extraction** As previously discussed in Section 4.1,  
 443 we proposed two methods for generating the  $(\text{noise}, \text{text})$  pairs for distillation: Sequential Ex-  
 444 traction, which generates new text via ancestral sampling from the teacher, and Parallel Extraction,  
 445 which recovers the posterior Gumbel noise from an existing text corpus. Although we have provided  
 446 theoretical support for the equivalence of these two methods, it still remains to be validated empiri-  
 447 cally whether Parallel Extraction works as well as Sequential Extraction in practice. Therefore, we  
 448 conduct ablation experiments by obtaining a dataset with the same size as LM1B via the sequential  
 449 method, and then train MDLM with and without Gumbel Distillation on this synthetic dataset.

450 Table 4 shows that Parallel Gumbel Extraction yields better performance than its sequential coun-  
 451 terpart, reducing generative perplexity from 86.38 to 67.64. This result may seem counterintuitive,  
 452 as sequential sampling generates data directly from the teacher’s distribution. We suppose that it  
 453 is susceptible to the teacher model’s own errors and biases. If the teacher generates repetitive or  
 454 low-quality text, the student will be trained to replicate these imperfections. In contrast, Parallel  
 455 Extraction leverages a high-quality, diverse text corpus as the ground truth for  $\mathbf{x}^{1:n}$ . It then uses the  
 456 teacher only to infer the posterior Gumbel noise  $\xi^{1:n}$  that would have led to the high-quality text.

457 **Impact of Gumbel vs. Other Noise Sources** Our method’s core principle is the deterministic  
 458 link between Gumbel noise and token probabilities established by the Gumbel-Max trick. To check  
 459 whether the specific properties of the Gumbel distribution are critical or harmful, we ablate our  
 460 approach by replacing it with two other noise sources. (1) **Gaussian Noise:** A standard random  
 461 signal commonly used in deep learning, which we transform Gumbel into and then feed as input;  
 462 (2) **Uniform Noise:** A particularly important baseline, as it is the precursor to Gumbel noise in  
 463 the inverse transform sampling procedure ( $\xi = -\log(-\log(u))$ ). This directly tests if the specific  
 464 transformation to the Gumbel distribution is necessary, or if any simple random variable is sufficient.

465 As shown in Table 4, both alternatives fail to match the performance of Gumbel noise. Using  
 466 Gaussian noise as the conditional signal significantly degrades performance, resulting in worse Gen.  
 467 PPL than the naive baseline. Using Uniform noise leads to training instability and mode collapse,  
 468 where the model generates extremely low-diversity text. The choice of Gumbel noise is fundamental  
 469 to creating a structured “blueprint” that the student model can effectively learn from.

## 471 6 CONCLUSION

472 In this work, we introduced Gumbel Distillation, a novel distillation framework designed to help  
 473 parallel decoders overcome their struggle to model the joint distribution of token sequences. By  
 474 using the Gumbel-Max trick to create a deterministic “blueprint” from an autoregressive teacher’s  
 475 sampling process, Gumbel Distillation reframes the intractable distribution matching problem into  
 476 a simple supervised task. Our experiments demonstrate that it is a versatile, plug-and-play module  
 477 that improves the quality, efficiency, and reasoning capabilities of diverse architectures like Mask  
 478 Diffusion Models and MTPs. Future work could involve scaling this technique to larger foundation  
 479 models and exploring the latent Gumbel space as a new avenue for controllable text generation.

480 **Limitation.** One limitation of this work is that as vocabulary size grows, the dimensionality of the  
 481 Gumbel noise vector increases proportionally. This can lead to higher computational costs and a  
 482 more challenging task in high-dimensional spaces. Future work could explore methods to mitigate  
 483 this, such as using structured or low-rank approximations for the Gumbel noise. Despite this, our  
 484 work paves the way for developing highly efficient generative models without compromising on  
 485 quality, making powerful generative AI more accessible for real-world applications.

486 REFERENCES  
487

488 Marianne Arriola, Aaron Gokaslan, Justin T Chiu, Zhihan Yang, Zhixuan Qi, Jiaqi Han, Sub-  
489 ham Sekhar Sahoo, and Volodymyr Kuleshov. Block diffusion: Interpolating between autoregres-  
490 sive and diffusion language models. In *International Conference on Learning Representations*,  
491 2025.

492 Jacob Austin, Daniel D Johnson, Jonathan Ho, Daniel Tarlow, and Rianne Van Den Berg. Structured  
493 denoising diffusion models in discrete state-spaces. *Advances in neural information processing*  
494 *systems*, 2021.

495 Yonatan Bisk, Rowan Zellers, Jianfeng Gao, Yejin Choi, et al. Piqa: Reasoning about physical com-  
496 monsense in natural language. In *Proceedings of the AAAI Conference on Artificial Intelligence*,  
497 2020.

498 Tom Brown, Benjamin Mann, Nick Ryder, Melanie Subbiah, Jared D Kaplan, Prafulla Dhariwal,  
499 Arvind Neelakantan, Pranav Shyam, Girish Sastry, Amanda Askell, et al. Language models are  
500 few-shot learners. In *Advances in neural information processing systems*, volume 33, pp. 1877–  
501 1901, 2020.

502 Tianle Cai, Yuhong Li, Zhengyang Geng, Hongwu Peng, Jason D Lee, Deming Chen, and Tri  
503 Dao. Medusa: Simple llm inference acceleration framework with multiple decoding heads. In  
504 *International Conference on Machine Learning*, pp. 5209–5235. PMLR, 2024.

505 Andrew Campbell, Joe Benton, Valentin De Bortoli, Thomas Rainforth, George Deligiannidis, and  
506 Arnaud Doucet. A continuous time framework for discrete denoising models. *Advances in Neural*  
507 *Information Processing Systems*, 35:28266–28279, 2022.

508 Ciprian Chelba, Tomas Mikolov, Mike Schuster, Qi Ge, Thorsten Brants, Philipp Koehn, and Tony  
509 Robinson. One billion word benchmark for measuring progress in statistical language modeling.  
2014.

510 Boyuan Chen, Diego Martí Monsó, Yilun Du, Max Simchowitz, Russ Tedrake, and Vincent Sitz-  
511 mann. Diffusion forcing: Next-token prediction meets full-sequence diffusion. *Advances in Neural*  
512 *Information Processing Systems*, 37:24081–24125, 2024.

513 Charlie Chen, Sebastian Borgeaud, Geoffrey Irving, Jean-Baptiste Lespiau, Laurent Sifre, and John  
514 Jumper. Accelerating large language model decoding with speculative sampling. *arXiv preprint*  
515 *arXiv:2302.01318*, 2023.

516 Ting Chen, Ruixiang Zhang, and Geoffrey Hinton. Analog bits: Generating discrete data using  
517 diffusion models with self-conditioning. *arXiv preprint arXiv:2208.04202*, 2022.

518 Christopher Clark, Kenton Lee, Ming-Wei Chang, Tom Kwiatkowski, Michael Collins, and Kristina  
519 Toutanova. Boolq: Exploring the surprising difficulty of natural yes/no questions. In *Proceedings*  
520 *of NAACL-HLT*, 2019.

521 Peter Clark, Isaac Cowhey, Oren Etzioni, Tushar Khot, Ashish Sabharwal, Carissa Schoenick, and  
522 Oyvind Tafjord. Think you have solved question answering? try arc, the ai2 reasoning challenge.  
523 *arXiv preprint arXiv:1803.05457*, 2018.

524 Arman Cohan, Franck Dernoncourt, Doo Soon Kim, Trung Bui, Seokhwan Kim, Walter Chang,  
525 and Nazli Goharian. A discourse-aware attention model for abstractive summarization of long  
526 documents. In *Proceedings of the 2018 Conference of the North American Chapter of the Asso-  
527 ciation for Computational Linguistics: Human Language Technologies, Volume 2 (Short Papers)*,  
528 pp. 615–621, 2018.

529 Gheorghe Comanici, Eric Bieber, Mike Schaeckermann, Ice Pasupat, Noveen Sachdeva, Inderjit  
530 Dhillon, Marcel Blstein, Ori Ram, Dan Zhang, Evan Rosen, et al. Gemini 2.5: Pushing the  
531 frontier with advanced reasoning, multimodality, long context, and next generation agentic capa-  
532 bilities. *arXiv preprint arXiv:2507.06261*, 2025.

533 DeepMind. Gemini diffusion. [https://deepmind.google/models/](https://deepmind.google/models/gemini-diffusion/)  
534 [gemini-diffusion/](https://deepmind.google/models/gemini-diffusion/), 2025.

540 Sander Dieleman, Laurent Sartran, Arman Roshannai, Nikolay Savinov, Yaroslav Ganin, Pierre H  
 541 Richemond, Arnaud Doucet, Robin Strudel, Chris Dyer, Conor Durkan, et al. Continuous diffu-  
 542 sion for categorical data. *arXiv preprint arXiv:2211.15089*, 2022.

543

544 Nima Fathi, Torsten Scholak, and Pierre-André Noël. Unifying autoregressive and diffusion-based  
 545 sequence generation. *arXiv preprint arXiv:2504.06416*, 2025.

546

547 Leo Gao, Jonathan Tow, Baber Abbasi, Stella Biderman, Sid Black, Anthony DiPofi, Charles Fos-  
 548 ter, Laurence Golding, Jeffrey Hsu, Alain Le Noac'h, Haonan Li, Kyle McDonell, Niklas Muen-  
 549 nighoff, Chris Ociepa, Jason Phang, Laria Reynolds, Hailey Schoelkopf, Aviya Skowron, Lintang  
 550 Sutawika, Eric Tang, Anish Thite, Ben Wang, Kevin Wang, and Andy Zou. The language model  
 551 evaluation harness, 07 2024. URL <https://zenodo.org/records/12608602>.

552

553 Itai Gat, Tal Remez, Neta Shaul, Felix Kreuk, Ricky TQ Chen, Gabriel Synnaeve, Yossi Adi, and  
 554 Yaron Lipman. Discrete flow matching. *Advances in Neural Information Processing Systems*, 37:  
 133345–133385, 2024.

555

556 Marjan Ghazvininejad, Omer Levy, Yinhan Yin, and Luke Zettlemoyer. Mask-predict: Parallel de-  
 557 coding of conditional masked language models. In *Conference on Empirical Methods in Natural  
 558 Language Processing (EMNLP)*, 2019.

559

560 Fabian Gloclekle, Badr Youbi Idrissi, Baptiste Rozière, David Lopez-Paz, and Gabriel Synnaeve.  
 561 Better & faster large language models via multi-token prediction. In *International Conference on  
 562 Machine Learning*, 2024.

563

564 Aaron Gokaslan and Vanya Cohen. Openwebtext corpus. [http://Skylion007.github.io/  
 565 OpenWebTextCorpus](http://Skylion007.github.io/OpenWebTextCorpus), 2019.

566

567 Shansan Gong, Mukai Li, Jiangtao Feng, Zhiyong Wu, and Lingpeng Kong. Diffuseq: Sequence  
 568 to sequence text generation with diffusion models. In *The Eleventh International Conference on  
 569 Learning Representations*, 2023.

570

571 Shansan Gong, Shivam Agarwal, Yizhe Zhang, Jiacheng Ye, Lin Zheng, Mukai Li, Chenxin An,  
 572 Peilin Zhao, Wei Bi, Jiawei Han, et al. Scaling diffusion language models via adaptation from  
 573 autoregressive models. In *International Conference on Learning Representations*, 2025.

574

575 Jiatao Gu, James Bradbury, Caiming Xiong, Victor OK Li, and Richard Socher. Non-autoregressive  
 576 neural machine translation. *arXiv preprint arXiv:1711.02281*, 2017.

577

578 Jiatao Gu, Chang Wang, and Jianbo Zhao. Levenshtein transformer. In *Advances in Neural Infor-  
 579 mation Processing Systems (NeurIPS)*, 2019.

580

581 Yuxian Gu, Li Dong, Furu Wei, and Minlie Huang. Minilm: Knowledge distillation of large lan-  
 582 guage models. *arXiv preprint arXiv:2306.08543*, 2023.

583

584 E.J. Gumbel. *Statistical Theory of Extreme Values and Some Practical Applications: A Series of  
 585 Lectures*. Applied mathematics series. U.S. Government Printing Office, 1954. URL <https://books.google.com/books?id=SNpJAAAAMAAJ>.

586

587 Xiaochuang Han, Sachin Kumar, and Yulia Tsvetkov. Ssd-lm: Semi-autoregressive simplex-  
 588 based diffusion language model for text generation and modular control. *arXiv preprint  
 589 arXiv:2210.17432*, 2022.

590

591 Zhengfu He, Tianxiang Sun, Kuanning Wang, Xuanjing Huang, and Xipeng Qiu. Diffusion-  
 592 bert: Improving generative masked language models with diffusion models. *arXiv preprint  
 593 arXiv:2211.15029*, 2022.

594

595 Jonathan Ho, Ajay Jain, and Pieter Abbeel. Denoising diffusion probabilistic models. *Advances in  
 596 neural information processing systems*, 2020.

597

598 Ari Holtzman, Jan Buys, Li Du, Maxwell Forbes, and Yejin Choi. The curious case of neural text  
 599 degeneration. In *International Conference on Learning Representations*, 2020.

594 Emiel Hoogeboom, Didrik Nielsen, Priyank Jaini, Patrick Forré, and Max Welling. Argmax flows  
 595 and multinomial diffusion: Learning categorical distributions. *Advances in neural information*  
 596 *processing systems*, 34:12454–12465, 2021.

597

598 Jungo Kasai, Jiatao Gu, Marjan Ghazvininejad, Luke Zettlemoyer, and Mohit Iyyer. A disentangled  
 599 context approach to non-autoregressive neural machine translation. In *International Conference*  
 600 *on Learning Representations (ICLR)*, 2021.

601 Jaeyeon Kim, Lee Cheuk-Kit, Carles Domingo-Enrich, Yilun Du, Sham Kakade, Timothy Ngo-  
 602 tiaoco, Sitan Chen, and Michael Albergo. Any-order flexible length masked diffusion. *arXiv*  
 603 *preprint arXiv:2509.01025*, 2025.

604

605 Wouter Kool, Herke van Hoof, and Max Welling. Stochastic beams and where to find them: The  
 606 gumbel-top-k trick for sampling sequences without replacement. In Kamalika Chaudhuri and  
 607 Ruslan Salakhutdinov (eds.), *International Conference on Machine Learning*, 2019.

608 Siqi Kou, Lanxiang Hu, Zhezhi He, Zhijie Deng, and Hao Zhang. Clms: Consistency large language  
 609 models. In *Forty-first International Conference on Machine Learning*, 2024.

610

611 Inception Labs, Samar Khanna, Siddhant Kharbanda, Shufan Li, Harshit Varma, Eric Wang, Sawyer  
 612 Birnbaum, Ziyang Luo, Yanis Miraoui, Akash Palrecha, et al. Mercury: Ultra-fast language  
 613 models based on diffusion. *arXiv preprint arXiv:2506.17298*, 2025.

614 Yaniv Leviathan, Matan Kalman, and Yossi Matias. Fast inference from transformers via speculative  
 615 decoding. In *International Conference on Machine Learning*, 2023.

616

617 Xiang Lisa Li, John Thickstun, Ishaan Gulrajani, Percy Liang, and Tatsunori Hashimoto. Diffusion-  
 618 lm improves controllable text generation. In *Advances in Neural Information Processing Systems*,  
 619 2022.

620 Yaron Lipman, Ricky TQ Chen, Heli Ben-Hamu, Maximilian Nickel, and Matt Le. Flow matching  
 621 for generative modeling. *arXiv preprint arXiv:2210.02747*, 2022.

622

623 Aixin Liu, Bei Feng, Bing Xue, Bingxuan Wang, Bochao Wu, Chengda Lu, Chenggang Zhao,  
 624 Chengqi Deng, Chenyu Zhang, Chong Ruan, et al. Deepseek-v3 technical report. *arXiv preprint*  
 625 *arXiv:2412.19437*, 2024a.

626 Anji Liu, Oliver Broadrick, Mathias Niepert, and Guy Van den Broeck. Discrete copula diffusion.  
 627 *arXiv preprint arXiv:2410.01949*, 2024b.

628

629 Lang Liu, Krishna Pillutla, Sean Welleck, Sewoong Oh, Yejin Choi, and Zaid Harchaoui. Diver-  
 630 gence Frontiers for Generative Models: Sample Complexity, Quantization Effects, and Frontier  
 631 Integrals. In *NeurIPS*, 2021.

632 Xingchao Liu, Chengyue Gong, and Qiang Liu. Flow straight and fast: Learning to generate and  
 633 transfer data with rectified flow. *arXiv preprint arXiv:2209.03003*, 2022.

634

635 Aaron Lou, Chenlin Meng, and Stefano Ermon. Discrete diffusion modeling by estimating the ratios  
 636 of the data distribution. In *International Conference on Machine Learning*, 2024.

637

638 Chris J. Maddison, Daniel Tarlow, and Tom Minka. A\* sampling. In *Advances in Neural Information*  
 639 *Processing Systems*. MIT Press, 2014.

640

641 Mitchell P. Marcus, Beatrice Santorini, and Mary Ann Marcinkiewicz. Building a large annotated  
 642 corpus of English: The Penn Treebank. *Computational Linguistics*, 19(2):313–330, 1993. URL  
 643 <https://aclanthology.org/J93-2004/>.

644

645 Stephen Merity, Caiming Xiong, James Bradbury, and Richard Socher. Pointer sentinel mixture  
 646 models. *arXiv preprint arXiv:1609.07843*, 2016.

647

648 Todor Mihaylov, Peter Clark, Tushar Khot, and Ashish Sabharwal. Can a suit of armor conduct  
 649 electricity? a new dataset for open book question answering. In *Proceedings of the Annual*  
 650 *Conference on Empirical Methods in Natural Language Processing*, 2018.

648 Shen Nie, Fengqi Zhu, Chao Du, Tianyu Pang, Qian Liu, Guangtao Zeng, Min Lin, and Chongxuan  
 649 Li. Scaling up masked diffusion models on text. *arXiv preprint arXiv:2410.18514*, 2024.  
 650

651 Shen Nie, Fengqi Zhu, Zebin You, Xiaolu Zhang, Jingyang Ou, Jun Hu, Jun Zhou, Yankai  
 652 Lin, Ji-Rong Wen, and Chongxuan Li. Large language diffusion models. *arXiv preprint*  
 653 *arXiv:2502.09992*, 2025.

654 Jingyang Ou, Shen Nie, Kaiwen Xue, Fengqi Zhu, Jiacheng Sun, Zhenguo Li, and Chongxuan Li.  
 655 Your absorbing discrete diffusion secretly models the conditional distributions of clean data. In  
 656 *International Conference on Learning Representations*, 2025.

657

658 D Paperno, G Kruszewski, A Lazaridou, QN Pham, Raffaella Bernardi, S Pezzelle, M Baroni,  
 659 G Boleda, and R Fernández. The lambada dataset: Word prediction requiring a broad discourse  
 660 context. In *54th Annual Meeting of the Association for Computational Linguistics, ACL 2016-  
 Long Papers*, volume 3, pp. 1525–1534. Association for Computational Linguistics (ACL), 2016.

661

662 William Peebles and Saining Xie. Scalable diffusion models with transformers. In *Proceedings of  
 663 the IEEE/CVF international conference on computer vision*, pp. 4195–4205, 2023.

664

665 Krishna Pillutla, Swabha Swayamdipta, Rowan Zellers, John Thickstun, Sean Welleck, Yejin Choi,  
 666 and Zaid Harchaoui. Mauve: Measuring the gap between neural text and human text using diver-  
 667 gence frontiers. *Advances in Neural Information Processing Systems*, 2021.

668

669 Alec Radford, Jeffrey Wu, Rewon Child, David Luan, Dario Amodei, and Ilya Sutskever. Language  
 670 models are unsupervised multitask learners. *OpenAI blog*, 18(9), 2019.

671

672 Subham Sahoo, Marianne Arriola, Yair Schiff, Aaron Gokaslan, Edgar Marroquin, Justin Chiu,  
 673 Alexander Rush, and Volodymyr Kuleshov. Simple and effective masked diffusion language  
 674 models. *Advances in Neural Information Processing Systems*, 2024.

675

676 Keisuke Sakaguchi, Ronan Le Bras, Chandra Bhagavatula, and Yejin Choi. Winogrande: An adver-  
 677 sarial winograd schema challenge at scale. *Communications of the ACM*, 2021.

678

679 Mohammad Samragh, Arnav Kundu, David Harrison, Kumari Nishu, Devang Naik, Minsik Cho, and  
 680 Mehrdad Farajtabar. Your llm knows the future: Uncovering its multi-token prediction potential.  
 681 *arXiv preprint arXiv:2507.11851*, 2025.

682

683 Andrea Santilli, Silvio Severino, Emilian Postolache, Valentino Maiorca, Michele Mancusi, Ric-  
 684 cardo Marin, and Emanuele Rodolà. Accelerating transformer inference for translation via paral-  
 685 lel decoding. *arXiv preprint arXiv:2305.10427*, 2023.

686

687 Jiaxin Shi, Kehang Han, Zhe Wang, Arnaud Doucet, and Michalis Titsias. Simplified and general-  
 688 ized masked diffusion for discrete data. *Advances in neural information processing systems*, 37:  
 689 103131–103167, 2024.

690

691 Makoto Shing and Takuwa Akiba. Diffusionblocks: Blockwise training for generative models via  
 692 score-based diffusion. *arXiv preprint arXiv:2506.14202*, 2025.

693

694 Jiaming Song and Linqi Zhou. Ideas in inference-time scaling can benefit generative pre-training  
 695 algorithms. *arXiv preprint arXiv:2503.07154*, 2025.

696

697 Jiaming Song, Chenlin Meng, and Stefano Ermon. Denoising diffusion implicit models. In *Inter-  
 698 national Conference on Learning Representations*, 2021.

699

700 Yuxuan Song, Zheng Zhang, Cheng Luo, Pengyang Gao, Fan Xia, Hao Luo, Zheng Li, Yuehang  
 701 Yang, Hongli Yu, Xingwei Qu, et al. Seed diffusion: A large-scale diffusion language model with  
 702 high-speed inference. *arXiv preprint arXiv:2508.02193*, 2025.

703

704 Jianlin Su, Murtadha Ahmed, Yu Lu, Shengfeng Pan, Wen Bo, and Yunfeng Liu. Roformer: En-  
 705 hanced transformer with rotary position embedding. *Neurocomputing*, 568:127063, 2024.

706

707 Haoran Sun, Lijun Yu, Bo Dai, Dale Schuurmans, and Hanjun Dai. Score-based continuous-time  
 708 discrete diffusion models. *arXiv preprint arXiv:2211.16750*, 2022.

702 Hugo Touvron, Thibaut Lavril, Gautier Izacard, Xavier Martinet, Marie-Anne Lachaux, Timothée  
 703 Lacroix, Baptiste Rozière, Naman Goyal, Eric Hambro, Faisal Azhar, et al. Llama: Open and  
 704 efficient foundation language models. *arXiv preprint arXiv:2302.13971*, 2023.

705

706 Ashish Vaswani, Noam Shazeer, Niki Parmar, Jakob Uszkoreit, Llion Jones, Aidan N Gomez,  
 707 Łukasz Kaiser, and Illia Polosukhin. Attention is all you need. In *Advances in neural information*  
 708 *processing systems*, volume 30, 2017.

709

710 Dimitri von Rütte, Janis Fluri, Yuhui Ding, Antonio Orvieto, Bernhard Schölkopf, and Thomas  
 711 Hofmann. Generalized interpolating discrete diffusion. In *International Conference on Machine*  
 712 *Learning*, 2025.

713

714 Guanghan Wang, Yair Schiff, Subham Sekhar Sahoo, and Volodymyr Kuleshov. Remasking discrete  
 715 diffusion models with inference-time scaling. In *ICLR Workshop on Deep Generative Model in*  
 716 *Machine Learning: Theory, Principle and Efficacy*, 2025.

717

718 Chengyue Wu, Hao Zhang, Shuchen Xue, Zhijian Liu, Shizhe Diao, Ligeng Zhu, Ping Luo, Song  
 719 Han, and Enze Xie. Fast-dllm: Training-free acceleration of diffusion llm by enabling kv cache  
 720 and parallel decoding. *arXiv preprint arXiv:2505.22618*, 2025.

721

722 Tong Wu, Zhihao Fan, Xiao Liu, Hai-Tao Zheng, Yeyun Gong, Jian Jiao, Juntao Li, Jian Guo, Nan  
 723 Duan, Weizhu Chen, et al. Ar-diffusion: Auto-regressive diffusion model for text generation.  
 724 *Advances in Neural Information Processing Systems*, 36:39957–39974, 2023.

725

726 Yisheng Xiao, Lijun Wu, Furu Meng, Tao Qin, and Tie-Yan Liu. A survey on non-autoregressive  
 727 generation for neural machine translation and beyond. *IEEE Transactions on Pattern Analysis*  
 728 *and Machine Intelligence*, 2022.

729

730 Minkai Xu, Tomas Geffner, Karsten Kreis, Weili Nie, Yilun Xu, Jure Leskovec, Stefano Ermon,  
 731 and Arash Vahdat. Energy-based diffusion language models for text generation. *arXiv preprint*  
 732 *arXiv:2410.21357*, 2024.

733

734 Jiacheng Ye, Zhihui Xie, Lin Zheng, Jiahui Gao, Zirui Wu, Xin Jiang, Zhenguo Li, and Lingpeng  
 735 Kong. Dream 7b: Diffusion large language models. *arXiv preprint arXiv:2508.15487*, 2025.

736

737 Rowan Zellers, Ari Holtzman, Yonatan Bisk, Ali Farhadi, and Yejin Choi. Hellaswag: Can a ma-  
 738 chine really finish your sentence? In *Proceedings of the Annual Meeting of the Association for*  
 739 *Computational Linguistics*, 2019.

740

741 Xiang Zhang, Junbo Zhao, and Yann LeCun. Character-level convolutional networks for text clas-  
 742 sification. *Advances in neural information processing systems*, 28, 2015.

743

744 Kaiwen Zheng, Yongxin Chen, Hanzi Mao, Ming-Yu Liu, Jun Zhu, and Qinsheng Zhang. Masked  
 745 diffusion models are secretly time-agnostic masked models and exploit inaccurate categorical  
 746 sampling. In *International Conference on Learning Representations*, 2024.

747

748 Lin Zheng, Jianbo Yuan, Lei Yu, and Lingpeng Kong. A reparameterized discrete diffusion model  
 749 for text generation. *arXiv preprint arXiv:2302.05737*, 2023.

750

751 Yuanzhi Zhu, Xi Wang, Stéphane Lathuilière, and Vicky Kalogeiton. Di[M]o: Distilling masked  
 752 diffusion models into one-step generator. *arXiv preprint arXiv:2503.15457*, 2025.

753

754

755

756 A USE OF LARGE LANGUAGE MODELS  
757

758 Regarding paper writing, we used LLM only for text polishing and grammar correction during  
759 manuscript preparation. No LLMs were involved in the conception or design of the method, ex-  
760 periments, or analysis. All technical content, results, and conclusions have been independently  
761 verified and validated by the authors. Apart from this, we also used LLM as an evaluation tool in  
762 our experiments to judge the generation quality of text samples.

764 B ON THE VALIDITY OF THE POSTERIOR GUMBEL SAMPLING METHOD  
765

766 In this section we give a formal proof of Theorem 4.1. Similar techniques on the posterior Gumbel  
767 distribution have been explored in prior works such as Kool et al. (2019), and we use some estab-  
768 lished findings from Maddison et al. (2014). Before proceeding with the proof, we first restate the  
769 full theorem from the main text.

770 **Theorem** (Posterior of the Gumbel-Max Process). *Assume  $X \in [V]$  is sampled from a set of logits  
771  $\mathbf{l} = (l_1, \dots, l_V) \in \mathbb{R}^V$  using the Gumbel-Max trick, such that  $X = \arg \max_{k \in [V]} (l_k + \xi_k)$ , where  
772  $\forall k, \xi_k \sim \mathcal{G}(0, 1)$  are i.i.d. standard Gumbel noises. Let  $p_k = \frac{\exp(l_k)}{\sum_j \exp(l_j)}$  be the softmax probability  
773 for each category  $k \in [V]$  and  $\xi = (\xi_1, \dots, \xi_V)$ . The posterior probability density function over  $\xi$   
774 conditioned on the outcome  $X = x$  is given by:*

$$776 p(\xi | X = x) = \frac{1}{p_x} \cdot \mathbf{1}_{\{g_x + \xi_x \geq g_k + \xi_k, \forall k \in [V]\}} \cdot \prod_{k=1}^V e^{-\xi_k - e^{-\xi_k}} \quad (1)$$

779 where  $\mathbf{1}_{\{\cdot\}}$  is the indicator function.

780 Furthermore, a sample  $\xi$  can be drawn from this posterior by first sampling auxiliary i.i.d. variables  
781  $\zeta_0, \dots, \zeta_V \sim \mathcal{G}(0, 1)$  and then applying the construction:

$$783 \xi'_k = \begin{cases} \zeta_0 - \log p_x & \text{if } k = x \\ -\log \left( \frac{\exp(-\zeta_k)}{p_k} + \exp(-\zeta_0) \right) & \text{if } k \neq x \end{cases} \quad (2)$$

785 This constructed sample  $\xi$  is guaranteed to have the following two properties:

787 1. (Condition satisfaction) The argmax of the perturbed logits matches the conditioned outcome.

$$788 \arg \max_{k \in [V]} (l_k + \xi'_k) = x$$

790 2. (Marginal Preservation) Each component of the sample is marginally a standard Gumbel.

$$791 \forall k \in [V], \quad \xi'_k \sim \mathcal{G}(0, 1)$$

793 B.1 PROOF OF PROPERTY 1  
794

795 *Proof.* We show that for any  $k \neq x$ , the inequality  $l_x + \xi'_x > l_k + \xi'_k$  holds. By substituting the  
796 construction formulas and the identity  $l_x - l_k = \log l_x - \log l_k$ , the inequality becomes:

$$797 (\log p_x - \log p_k) + \zeta_0 - \log p_x > -\log \left( \frac{\exp(-\zeta_k)}{p_k} + \exp(-\zeta_0) \right)$$

$$799 -\log p_k + \zeta_0 > -\log \left( \frac{\exp(-\zeta_k)}{p_k} + \exp(-\zeta_0) \right)$$

$$801 \zeta_0 > \log \left( \frac{p_k}{\frac{\exp(-\zeta_k)}{p_k} + \exp(-\zeta_0)} \right)$$

805 Exponentiating both sides and rearranging yields:

$$806 \frac{e^{\zeta_0 - \zeta_k}}{p_k} + 1 > p_k$$

808 This inequality holds because the left-hand side is always strictly greater than 1, while  $p_k \in [0, 1]$ .  $\square$

810 B.2 PROOF OF PROPERTY 2  
811812 We prove that each component of the constructed sample  $\xi'_k$  is marginally distributed as a standard  
813 Gumbel,  $\mathcal{G}(0, 1)$ . We handle the winning ( $k = x$ ) and losing variables ( $k \neq x$ ) separately.  
814815 CASE 1: THE WINNING VARIABLE ( $\xi_x$ )  
816817 *Proof.* The proof for the winning variable's marginal distribution relies on the **Posterior of the**  
818 **Maximum** property of the Gumbel distribution (Maddison et al., 2014). This property states that  
819 the maximum score,  $M = \max_{k \in [V]} (l_k + \xi_k)$ , conditioned on the winning category being  $x$ , follows  
820 a Gumbel distribution centered at the winning logit  $l_x$ :  
821

822 
$$p(M \mid \arg \max_{k \in [V]} (l_k + \xi_k) = x) \sim \mathcal{G}(l_x, 1)$$

823 The posterior construction is equivalent to a top-down sampling process where a sample of the  
824 maximum score, call it  $m^*$ , is first drawn from this posterior distribution. Thus,  $m^* \sim \mathcal{G}(l_x, 1)$ .  
825826 By definition,  $m^*$  must be equal to the score of the winning category from our constructed sample:  
827

828 
$$m^* = l_x + \xi'_x$$

829 By rearranging the equation, we can express the constructed Gumbel noise  $\xi_x$  in terms of  $m^*$ :  
830

831 
$$\xi_x = m^* - l_x$$

832 Since  $m^*$  is a randomly sampled from  $\mathcal{G}(l_x, 1)$ , subtracting the location parameter  $l_x$  simply shifts  
833 the distribution's location to zero. Therefore, the resulting random variable  $\xi_x$  follows:  
834

835 
$$\xi_x \sim \mathcal{G}(l_x - l_x, 1) = \mathcal{G}(0, 1)$$

836 Thus, the marginal distribution of any winning variable  $\xi_x$  is the standard Gumbel distribution.  $\square$   
837838 CASE 2: THE LOSING VARIABLE ( $\xi_k, k \neq x$ )  
839840 *Proof.* The proof for the losing variables is more involved. We show that the cumulative distribution  
841 function (CDF) of  $\xi_k$  for any  $k \neq x$  matches the standard Gumbel CDF,  $F(t) = e^{-e^{-t}}$ .  
842843 The construction formula for a losing variable is:  
844

845 
$$\xi_k = -\log \left( \frac{\exp(-\zeta_k)}{p_k} + \exp(-\zeta_0) \right)$$

846 The proof proceeds with a change of variables. We use the property that if  $\zeta \sim \mathcal{G}(0, 1)$ , then its  
847 transformation  $U = e^{-\zeta}$  follows the standard Exponential distribution,  $U \sim \text{Exponential}(1)$ . Let  
848  $U_k = e^{-\zeta_k}$  and  $U_0 = e^{-\zeta_0}$ . Both are i.i.d. samples from Exponential(1).  
849850 The CDF,  $P(\xi_k \leq t)$ , is equivalent to the probability  $P\left(\frac{U_k}{p_k} + U_0 \geq e^{-t}\right)$ . This probability is found  
851 by integrating the joint PDF of  $U_k$  and  $U_0$ , which is  $f(u_k, u_0) = e^{-u_k} e^{-u_0}$  for  $u_k, u_0 \geq 0$ , over the  
852 region satisfying the inequality. Letting  $c = e^{-t}$ , the integral is:  
853

854 
$$P(\xi_k \leq t) = \int_0^\infty \int_0^\infty \mathbf{1}_{\left\{ \frac{u_k}{p_k} + u_0 \geq c \right\}} e^{-u_k} e^{-u_0} du_k du_0$$

855 While we omit the full integration here for brevity, it simplifies to the CDF (Maddison et al., 2014).  
856

857 
$$P(\xi_k \leq t) = e^{-c} = e^{-e^{-t}}$$

858 Thus, the marginal distribution of any losing variable  $\xi_k$  is the standard Gumbel distribution.  $\square$   
859860 C EXPERIMENTAL DETAILS  
861862 C.1 MASKED DIFFUSION LANGUAGE MODELS  
863864 **MDLM and BD3-LM** Text diffusion models (Austin et al., 2021; Li et al., 2022) extend diffusion  
865 from visual domains to language modeling. The design is to reverse a forward process  $q$  that gradually  
866 corrupts clean text into noise, which can use continuous or discrete representations. A denoising

864 model  $p_\theta$  is trained to recover the original text  $x$  from a noisy version  $x_t$  where  $t \in [0, 1]$  is the noise  
 865 level. The learning objective is typically the minimization of the Negative Evidence Lower Bound  
 866 (NELBO), which can be expressed in a simplified form as:

$$868 -\log p_\theta(x) \leq \mathcal{L}_{\text{NELBO}}(x; \theta) = \mathbb{E}_{t, x_t \sim q(\cdot | x)} [-w(t) \cdot \log p_\theta(x | x_t)], \quad (3)$$

870 A prominent family of text diffusion models uses masking as the corruption process. Masked Diffusion  
 871 Language Model (MDLM) (Sahoo et al., 2024) is a simple yet effective architecture that learns  
 872 to predict original tokens given a partially masked sequence. However, MDLM is designed only  
 873 for fixed-length generation. To address this, Block Discrete Denoising Diffusion Language Model  
 874 (BD3-LM) (Arriola et al., 2025) extends the idea by interpolating between diffusion and AR models.  
 875 It generates text autoregressively over blocks of tokens, but within each block, it uses a diffusion  
 876 process identical to that of MDLM. This hybrid approach enables variable-length generation. Be-  
 877 cause the core objective within a block is the same for both models, we use the simpler MDLM  
 878 architecture for illustration in Figure 5, but use the full BD3-LM objective for our derivations below.

879 The BD3-LM objective factorizes the loss across  $B$  blocks as follows:

$$880 \mathcal{L}_{\text{NELBO}}(x^{1:n}; \theta) = \sum_{b=1}^B \mathcal{L}_{\text{NELBO}}(x^{(b-1)c+1:bc} | x^{\leq(b-1)c}; \theta). \quad (4)$$

883 Here, the loss for each block is conditioned on the clean, previously generated blocks.

884 We adapt this block-wise objective to be conditioned on our Gumbel signal. The overall task is  
 885 to learn the conditional distribution  $p_\theta(x^{1:n} | \xi^{1:n})$ , and we achieve this by modifying the BD3-LM  
 886 objective from Equation 4, adding the corresponding slice of the Gumbel sequence as a condition  
 887 for each block. This results in a conditional NELBO:

$$888 \mathcal{L}_{\text{NELBO}}(x^{1:n} | \xi^{1:n}; \theta) = \sum_{b=1}^B \mathcal{L}_{\text{NELBO}}(x^{(b-1)c+1:bc} | x^{\leq(b-1)c}, \xi^{(b-1)c+1:bc}; \theta). \quad (5)$$

889 As mentioned in Section 4.2, a crucial implementation detail is how the Gumbel signal  $\xi^{1:n}$  is  
 890 injected into the model. In practice, we process the raw Gumbel noise for each block,  $\xi^b$ , into a dense  
 891 vector on the embedding space,  $g(\xi^b)$ , by first performing a softmax operation for normalization,  
 892 followed by a learned linear projection. Then we use to replace the embeddings of [MASK] tokens  
 893 in the noised input. Formally, let  $E(x_t^b)$  be the initial token embeddings for a noised block  $b$ , let  $M^b$   
 894 be a binary mask where  $M_i^b = 1$  if the  $i$ -th token is [MASK] and 0 otherwise, and let  $W_{\text{proj}}$  be the  
 895 weight matrix of the linear layer. Then, the final input to the model’s transformer layers,  $\tilde{E}(x_t^b)$ , is:

$$896 \tilde{E}^b = (1 - M^b) \odot E(x_t^b) + M^b \odot g(\xi^b) \quad \text{where} \quad g(\xi^b) = \text{softmax}(\xi^b) W_{\text{proj}}. \quad (6)$$

900 Here  $\odot$  denotes element-wise multiplication. This design substitutes the uninformative [MASK]  
 901 embeddings with Gumbel signals, which serve as a “blueprint” for what to predict at those positions.  
 902 In Figure 5, we give an illustration of how Gumbel Distillation is integrated into MDLM.

903 **Datasets** Following Sahoo et al. (2024); Arriola et al. (2025), we conduct our experiments on  
 904 two datasets, The One Billion Word Dataset; **LM1B** (Chelba et al., 2014) and OpenWebText;  
 905 **OWT** (Gokaslan & Cohen, 2019). We use a context length of 128 for models trained on LM1B  
 906 and 1024 for models trained on OWT. For both datasets, we use the GPT-2 tokenizer to keep con-  
 907 sistent with our selected teacher model. For LM1B, sequences were concatenated and wrapped to  
 908 a maximum length of 128. For OWT, documents were concatenated and chunked into sequences of  
 909 1,024 tokens, with an [eos] token used as a separator between documents. Since OWT does not have  
 910 an official validation split, we created one by holding out the last 100,000 documents.

911 **Model Architectures and Baselines** We use GPT-2-Large as teacher model for MDLM and BD3-  
 912 LM, both of which augments the diffusion transformer (Peebles & Xie, 2023) with rotary positional  
 913 embeddings (Su et al., 2024). All model (including the AR baseline) implementation follows the  
 914 transformer architecture from Arriola et al. (2025) that uses 12 layers, a hidden dimension of 768,  
 915 and 12 attention heads, which corresponds to 110M parameters (excluding embeddings).

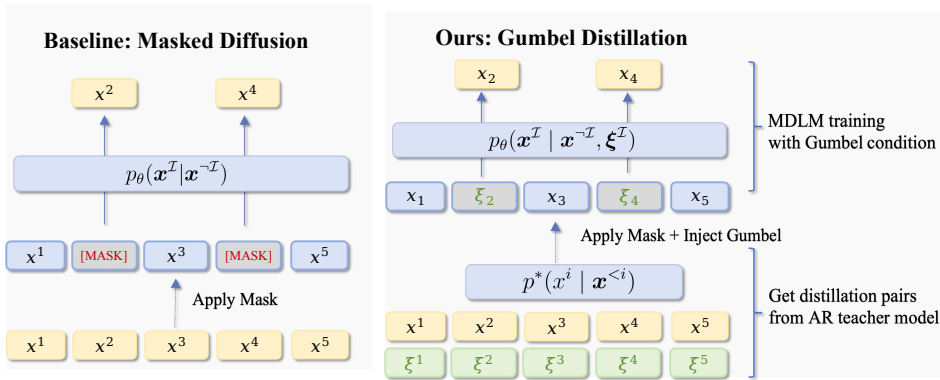


Figure 5: Gumbel Distillation Integrated with MDLM. Left: original MDLM architecture, masked positions are predicted based solely on the unmasked context. Right: Gumbel-conditioned architecture: distillation pairs  $(\xi, x)$  are obtained from an AR teacher; then MDLM is modified to take Gumbel as conditional input, learning to predict masked positions with corresponding Gumbel noise.

**Training** All models were trained for 1 million steps using the AdamW optimizer with a batch size of 512, and a constant learning rate of  $3 \times 10^{-4}$  with a 2,500-step linear warmup. This translates to 65B tokens and 73 epochs on LM1B, 524B tokens and 60 epochs on OWT. For BD3-LM, we follow the baseline by training with maximum context length first for 850K gradient steps (effectively the same as MDLM) then fine-tune on the target block size for 150K gradient steps. We maintain consistent random seeds to ensure fair comparisons. All experiments are run on H100 GPUs.

**Nucleus Sampling** For all baselines, we follow their default setup and employ nucleus sampling (Holtzman et al., 2020) with  $p = 0.9$ . As discussed in many prior works (von Rütte et al., 2025; Wang et al., 2025), one could get suspiciously low generative perplexity values as  $p$  becomes very small, at the cost of sacrificing diversity/entropy. We noticed that for models trained with Gumbel Distillation, the diversity of the samples is more robust against low  $p$  values than the baseline, which could be attributed to the stochasticity brought by the randomly drawn Gumbel as the conditional input. To keep consistent with the baselines, we still use  $p = 0.9$  for Gumbel-conditioned models.

**Gumbel-based Categorical Sampling for Diffusion Models** Zheng et al. (2024) analyzed the numerical issues of Gumbel-based categorical sampling for diffusion models and offered two methods for improvement, including (1) sampling 64-bit Gumbel variables instead of 32-bit to reduce the truncation effect, and (2) using their proposed first-hitting sampler. The BD3-LM baseline adopts both methods, which we choose to follow in our experiments.

However, it is worth noting that (1) Zheng et al. (2024) points out the token-by-token decoding process of masked diffusion models by their first-hitting sampler does not suffer from notable numerical issues under 32-bit precision, which makes it unnecessary to adopt both methods at the same time, and (2) the first-hitting sampler effectively limits the masked diffusion model to unmask one token at each step, making its inference cost the same as AR models. Therefore, when we obtain samples using fewer NFEs than the generated sequence length, first-hitting is disabled and we fall back to the efficient ancestral sampler from Sahoo et al. (2024).

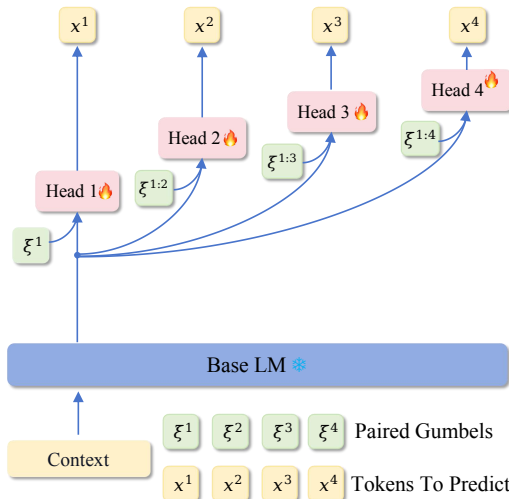
**Inference with Calibrated Gumbel Noise** During training, the Gumbel noise  $\xi$  is drawn from  $\mathcal{G}(0, 1)$  to fully capture the teacher’s sampling variance. At inference, however, we observe that the heavy tails of Gumbel can occasionally produce rare, high-magnitude values that can lead to lower-quality samples. To ensure more stable and reliable generation, we can draw from a calibrated Gumbel distribution by introducing a temperature parameter  $\tau \in (0, 1]$  and scaling the guidance as  $\xi \rightarrow \xi * \tau$  from the same Gumbel family but with a reduced variance, effectively controlling the influence of extreme values. Empirically, a slightly reduced temperature is found to bring substantial improvement in generative perplexity with minor decline in entropy, indicating that guidance from a lower-variance distribution is more consistently reliable. In our experiments, we use  $\tau = 0.85$ .

972 C.2 MULTI-TOKEN-PREDICTION  
973

974 **Medusa** Prior to Medusa (Cai et al., 2024), various speculative decoding strategies (Leviathan  
975 et al., 2023; Chen et al., 2023) have been proposed to reduce the number of decoding steps for  
976 LLMs, where a smaller draft model is used to generate a token sequence, which is then refined  
977 by the original larger model for acceptable continuation. Instead, Medusa proposes using multiple  
978 decoding heads on top of the backbone model to expedite inference. These are additional decoding  
979 heads appended to the last hidden states of the original model. Specifically, given the original  
980 model’s last hidden states  $h_t$  at position  $t$ ,  $K$  decoding heads are added to  $h_t$ . The  $k$ -th head is used  
981 to predict the token in the  $(t+k+1)$ -th position (the original language model head is used to predict  
982 the  $(t+1)$ -th position). A single layer of feed-forward network with a residual connection is used  
983 for each head. Denote the prediction of the  $k$ -th head as  $p_t^{(k)}$ , then the definition of the  $k$ -th head is:  
984

$$985 p_t^{(k)} = \text{softmax} \left( W_2^{(k)} \cdot \left( \text{SiLU}(W_1^{(k)} \cdot h_t) + h_t \right) \right), \text{ where } W_2^{(k)} \in \mathbb{R}^{d \times V}, W_1^{(k)} \in \mathbb{R}^{d \times d}. \quad (7)$$

986  $d$  is the output dimension of the LLM’s last hidden layer and  $V$  is the vocabulary size.  $W_2^{(k)}$   
987 is initialized identically to the original language model head, and  $W_1^{(k)}$  to zero, which aligns the  
988 initial prediction of the heads with the original model. The heads are trained in conjunction with  
989 the original backbone model, which can be frozen (Medusa-1) or trained together (Medusa-2). At  
990 inference, a tree-structured attention mechanism is employed to process multiple candidates from  
991 each head concurrently. Empirically, Medusa found that five heads are sufficient at most.  
992



1009 Figure 6: Gumbel Distillation integrated with Medusa. The base backbone model is frozen when  
1010 training the MTP heads. We first obtain distillation pairs  $(\xi, x)$  from the AR backbone as teacher,  
1011 then each MTP head is modified to take Gumbel as conditional input.  
1012

1013 **Model Architecture** For simplicity and consistency with our other experiments, we choose GPT-  
1014 2-Small as the backbone and follow Medusa-1’s setup to freeze the backbone model during training.  
1015 Since the open-source code of Medusa mainly supports certain LLMs, we re-implemented the core  
1016 framework for our controlled-scale experiments on GPT-2-Small. As shown in Figure 6, we select  
1017 the number of MTP heads as 4. Since each MTP head is designed to be a single linear layer, we first  
1018 normalize and project Gumbel vectors via the same process as described for MDLMs, then we accu-  
1019 mulate the Gumbel sequence via a small causal transformer and feed its output to the corresponding  
1020 hidden state slice from the backbone as a condition for each head.  
1021

1022 **Training and Inference** We simulate a self-distillation setup, adopting the assumption that Open-  
1023 WebText (Gokaslan & Cohen, 2019) matches GPT-2’s output distribution. The MTP prediction  
1024 heads are trained with a batch size of 256 for 20K steps as we observe further training does not  
1025 improve the performance as much. At inference, we follow Medusa-1’s setup and adopt typical  
acceptance as the strategy for speculative decoding, where the proposal is verified against both a

1026 hard probability threshold and a soft entropy-dependent threshold. Specifically, given  $x_1, \dots, x_n$  as  
 1027 context, when evaluating the candidate sequence  $x_{n+1}, \dots, x_{n+k}$ , a candidate is accepted when:  
 1028

$$p_{\text{original}}(x_{n+k} \mid x_1, x_2, \dots, x_{n+k-1}) > \min(\epsilon, \delta \exp(-H(p_{\text{original}}(\cdot \mid x_1, x_2, \dots, x_{n+k-1})))) \quad (8)$$

1029 We select  $\epsilon = 0.1$  and  $\delta = 1.0$  for our experiments. To evaluate the acceptance rates, we adopt a  
 1030 simple sequential strategy and verify each candidate only when all previous candidates have been  
 1031 accepted. We randomly select beginning slices of samples from the validation set of OWT and let  
 1032 the MTP heads complete after the starting prompt. Reported results are averaged over 500 samples.  
 1033

## 1035 D EVALUATION DETAILS

### 1038 D.1 ON EVALUATING GENERATIVE QUALITY OF DIFFUSION LANGUAGE MODELS

1039 To quantitatively assess models’ performance, we adopt standard language modeling metrics. For  
 1040 unconditional text generation, our primary metric is **Generative Perplexity (Gen. PPL)**, evaluated  
 1041 using a pre-trained GPT-2-Large model. Since GPT2-Large uses a context size of 1024, we follow  
 1042 our baselines and compute Gen. PPL for samples longer than 1024 tokens using a sliding window  
 1043 with a stride length of 512. The numbers reported are an average of 300 generated samples.

1044 In addition to Gen. PPL, we also follow recent works (Wang et al., 2025; Fathi et al., 2025; Shing  
 1045 & Akiba, 2025) to report the **MAUVE score** (Liu et al., 2021). While Gen PPL is a commonly  
 1046 used metric for measuring fluency, it can be an unreliable indicator of overall quality as it often fails  
 1047 to capture crucial aspects like diversity and creativity. A model can achieve lower perplexity score  
 1048 by generating repetitive or overly generic text that is highly probable under the reference model,  
 1049 yet this does not correlate well with human judgments of quality. In comparison, MAUVE score  
 1050 provides a more comprehensive assessment by comparing the distribution of model-generated text  
 1051 against the distribution of human text, offering a balance between generation quality and diversity  
 1052 that cannot be “hacked” by tuning sampling hyperparameters. Following Pillutla et al. (2021), we  
 1053 compute MAUVE score with 5000 samples from the validation set of OWT as the reference data.

### 1055 D.2 ZERO-SHOT BENCHMARKS

1056 For downstream performance evaluation, we use the `lm-eval-harness` (Gao et al., 2024) library  
 1057 which allows custom models to run on benchmarks by providing likelihood estimation and text  
 1058 generation APIs. For likelihood-based multiple-choice tasks, we compute per-token likelihood over  
 1059 both context and completion (excluding padding). We adopt one-step evaluation, as this tests pure  
 1060 generative capacity without partial information, providing deterministic low-variance estimates that  
 1061 give more stable and discriminative results. The models perform one forward pass on the input  
 1062 where only answer completion tokens are masked, and the likelihood for each token is extracted from  
 1063 the model’s predictions at the masked positions. For BD3-LM, block boundaries are respected by  
 1064 sequentially masking entire aligned blocks. Sequences exceeding model length are right-truncated  
 1065 to maintain recent context, similar to autoregressive context scrolling.

### 1067 D.3 LLM-AS-JUDGE

1068 Following previous work (von Rütte et al., 2025), we evaluate the quality of the unconditionally  
 1069 generated text samples by using LLM as a judge. Specifically, we employ the Gemini 2.5 pro API  
 1070 (Comanici et al., 2025) to rate the samples based on clarity, diversity and fluency on a scale of 1 to  
 1071 10. We provide the sample text along with instructions for the LLM to first give a justification and  
 1072 then grade each dimension accordingly. The final output from the LLM is restricted to a json format  
 1073 for parsing. See Figure 7 for the prompt template we used to instruct the LLM for the evaluation.

## 1076 E ADDITIONAL RESULTS

### 1078 E.1 MAZE NAVIGATION TOY

1079 Here we present more details on the maze navigation toy’s setup and results.

```

1080
1081 You are an expert text quality evaluator. Please evaluate the given text sample from
1082 these dimensions using a 1-10 scale with decimal precision.
1083
1084 1. Clarity: Assess how clear and logical the text is; Consider:
1085   - Is the main message/topic clear?
1086   - Do ideas flow logically from one to the next?
1087   - Is the text easy to follow and comprehend?
1088   Note: Text may be an excerpt, don't penalize incomplete context.
1089 2. Grammaticality: Evaluate grammatical correctness; Consider:
1090   - Proper sentence structure and syntax
1091   - Correct use of punctuation, capitalization
1092   - Subject-verb agreement, tense consistency
1093   - Absence of grammatical errors
1094 3. Factuality: Assess accuracy of verifiable information; Consider:
1095   - Are stated facts (dates, names, places, numbers) accurate?
1096   - Does information align with common knowledge?
1097   - If no verifiable facts present, score based on plausibility.
1098   - Focus on internal consistency rather than perfect accuracy
1099 4. Style: Evaluate the quality of writing style and fluency; Consider:
1100   - Sentence variety and rhythm
1101   - Appropriate vocabulary and word choice
1102   - Natural flow and readability
1103   - Professional/appropriate tone for the content type
1104 5. Creativity : Assess creative and engaging qualities; Consider:
1105   - Original ideas, unique perspectives, or interesting approaches
1106   - Engaging language and expression
1107   - Creative use of language, metaphors, or descriptions
1108   - Avoidance of overly generic content
1109
1110 The text to be graded is as follows:
1111 """
1112 {text}
1113 """

```

Figure 7: Prompt used for LLM-based evaluation using Gemini-2.5-pro.

As shown in Figure 2, we used a  $5 \times 4$  map for the maze. Denote the coordinate of the upper left point as  $(0, 0)$ , our start point is set to  $(3, 1)$  and target point is set to  $(3, 4)$ . Given a vocabulary of,  $\{\text{<bos>}, \text{<eos>}, \text{up}, \text{down}, \text{left}, \text{right}\}$ , we define a simple language as a sequence of actions that form a valid path from start to target in the maze, and set the maximum path length is to 10. We used BFS to generate 2000 valid paths as the training dataset.

For the AR model, its architecture is a transformer with 8 layers, 8 heads and a dimension of 128. We trained it with a batch size of 256 and learning rate of 3e-4 for 200 epochs to obtain an “ideal” teacher that almost always generates valid paths. Then, we implemented a simplified version of MDLM as student and trained it with/without Gumbel Distillation using the AR model as teacher. The student model is a transformer with 4 layers, 4 heads and a dimension of 128, and was also trained with a batch size of 256 and learning rate of 3e-4 for 200 epochs. At inference, we generate 100 paths using different number of steps and count the number of successful generations. For AR, NFE is fixed at 10 whereas we try NFE=1,2,4,8 and 16 for MDLM. The success rates are below:

Table 5: Success rates vs. NFEs for MDLM and MDLM + Gumbel Distillation on the maze toy.

| NFE                        | =1          | =2          | =4          | =8          | =16         |
|----------------------------|-------------|-------------|-------------|-------------|-------------|
| MDLM                       | 53.0        | 64.0        | 69.0        | 81.0        | 94.0        |
| MDLM + Gumbel Distillation | <b>82.0</b> | <b>86.0</b> | <b>97.0</b> | <b>99.0</b> | <b>98.0</b> |

## E.2 LIKELIHOOD ESTIMATION

In Table 6, we also report the zero-shot validation perplexities. We evaluate the likelihood of models trained with OWT on Penn Tree Bank (PTB; (Marcus et al., 1993), WikiText (Merity et al., 2016), LM1B, Lambada (Paperno et al., 2016), AG News (Zhang et al., 2015) and Scientific Papers (Pubmed and Arxiv subsets) (Cohan et al., 2018). Since the zeroshot datasets have different conventions for sequence segmentation, we wrap sequences to 1024 and do not add eos tokens.

Note that the results here are *heavily* biased towards models trained with Gumbel Distillation as they are conditioned on the Gumbel vectors corresponding to the ground truth sequences. Since the

1134 model has learned a mapping from Gumbel noises to coherent AR outputs, it can generate good text  
 1135 samples using random Gumbel at inference, but this does not guarantee the prediction of the exact  
 1136 sequence on the validation set. However, we believe these results demonstrate how well the model  
 1137 has learned to estimate the conditional likelihood when the exact corresponding Gumbel is given.  
 1138

1139 Table 6: Validation perplexities ( $\downarrow$ ) of models trained on OWT.  
 11401141 

## F GENERATION SAMPLES

1142  
 1143  
 1144  
 1145  
 1146  
 1147  
 1148  
 1149  
 1150  
 1151     <|endoftext|>The two Houses have adopted a bipartisan approach, inviting new rules and  
 1152     licensing releases for federal agencies. Currently, they require the agencies to have  
 1153     in-depth internal review of the rules. They agreed on rules and didn't stop until Banking  
 1154     and Budget Chairmen shared the Senate Finance Act through Senate Finance Bill 2012,  
 1155     though there is no immediate support for any reform. Democrats are not united in wanting  
 1156     a near-complete return to the rules, which would require months of political pressure to  
 1157     rein in regulators. While some Republicans now have pre-existing differences, Majority  
 1158     Chairman Jim Cantor (R-West Virginia) has softened his stance. He said the House will  
 1159     continue support committee work on a bill to help break the rules but also create a  
 1160     complex overhaul. But Mr. Cantor said that, I sort of implicitly trust that we will pass  
 1161     the bills in a bipartisan way with unified Republican leadership. Still, Democrats  
 1162     continue to be cautious about what it would cost for the 2012 financial bill to pass. Mr.  
 1163     Cantor's measure is to be the final one that cleared the Senate next week. The House will  
 1164     return it on the floor for consideration if it passes rules, Mr. Dehner promised. Senators  
 1165     and Republicans say they never expressed support for much more oversight of federal  
 1166     regulators because of the controversial Dodd-Frank overhaul in late 2013. Democrats had  
 1167     resisted plans for several other Dodd-Frank initiatives to go beyond the beltway and  
 1168     create a line for federal oversight. They feared that financial regulators would set up a  
 1169     revolving door and endless financial-related regulations could slow data collections and  
 1170     satisfy people. But Senator Daniel D. Coats (R-Ohio) offered flat tax increases to create  
 1171     the height-line approach. Now, the idea is are regulatory overhauls, Financial Services  
 1172     Chairman John Thune said Additional reporting by Benjamin Reeves<|endoftext|>By Edward  
 1173     Snowden: Susan Onghi Kara CORRECTION: John Tonex says ""Uhoh pills"" on record. Forty to  
 1174     2, Edward Snowden. SiriusXM Broadcast A few days ago, Frank Geithner spoke on The Friends  
 1175     Hour of 11 News Bloomberg about defending the ground line in the fight against Pragmatism  
 1176     and saying that the only alternative in the matter requires a reading of the Elements  
 1177     Policy of Medics. Neither, though, should draw a line on important and essential issues. He  
 1178     said that an alternative is necessary after an important decision stage for Russia.  
 1179     Vitaliy Goldifkin earlier had outlined a set of decisions with major implications.  
 1180     Russia's actions will risk a layer of sanctions and the ire of many Republicans in  
 1181     Congress. He warned that regional actors are in conflict on a wide level, saying that the  
 1182     West perceives that power and influence grandly come to dictate strategic posture,  
 1183     economic, military, and political determination. He passed on saying except tranquility  
 1184     with regards to the nuclear weapons regime, there could be a result of direct, direct  
 1185     disruption of the Russian economy. But after just enough debate and more explanation, it  
 1186     had emerged: The treaty must renew and be upheld. Ultimately, the United States must rely  
 1187     upon our allies to sift through the facts. Russia made the nuclear commitment publicly,  
 1188     on the possibility of a possible joint military strike. Nevertheless, any type of action,  
 1189     through the physical and through the enforcement of the treaty, is a priority of the  
 1190     United States, Rouhani said. The European Union have already indicated they would punish  
 1191     Russia with a retaliatory measure, Russia would impose other sanctions, and far China  
 1192     China look to develop an immediate utter surprise of retaliation, considering China's  
 1193     economic policy, which applies if Putin seeks it. Putin talked like way about a potential  
 1194     reshuffle of Saudi Arabia and Iran. The Saudis themselves could just show their  
 1195     belligerence toward Russia or encourage the United States to use force to quickly squeeze  
 1196     Russia. But Obama has given the Saudis an excuse to berate them diplomatically for  
 1197     slippage, while relish to suggest that the United States is consummate engaged in  
 1198     sanctions against Russia. That situation continues with the Russian response. The report  
 1199     that Russia is about to install a nuclear missile shield on U.S. One waves the Twitter  
 1200     prompting of unnamed Russian statesman Andrei Lavrov. Others chimed ramefully by sounding  
 1201     the following bell. Its not gained from you. Author Vashemi Kopacak stepped in for Putins  
 1202     explanation. That disregards what you sent over cross borders with your hands, what you  
 1203     chose to eat and listen to strangers while people at or having intel leak out to your  
 1204     enemies. Why they cant you put your weapons to the enemy and calculate it. No'

1184 Figure 8: Sample from MDLM of length 1024 and T = 1024 steps. The generative perplexity of the  
 1185 sample under GPT-2-Large is 62.36 and its entropy is 5.56.  
 1186

1187

1188

1189

1190

1191

1192

1193

1194

1195

1196

1197

The Japan Galactic Institute has announced that it will become the world's ever-growing space lab. The company will be developing a commercial system and used to move Japan's space ship into the next frontier. The market is booming and the central Japanese market forecasts revenues of \$2.6 billion to \$3.8 billion in 2013. "Japan Galactic is a big step forward in getting used to in Japan, which has the ability to be the biggest of the world," said Jean Phillips, chief executive of European Science Systems (ASES), an international research company. "As for the Japanese government's success in foreign policy, we're proud that the CNAS is a partner. We look like the Japan Galactic Institute is a huge step to something of a world-type science laboratory." Kashisei and its partners have been developing Japan as a global hub for industries such as solar power and tourism. Starting in the early 1990s, Japan saw building towns, cities, villages, towns, rural areas and villages a quarter to a quarter and a third of the world's GDP. In 2010, the Nordic country recorded an annual GDP of \$1.11 billion and grew by \$14.1 billion faster than originally projected. Japan's global GDP grew to \$14.8 billion, \$181 million in 2013, and \$130 million, with Asian nations slowly adopting new varieties of seed for crops and indigenous seeds for their own growing economies. That's because Japan has managed to use the technology to get a website for online courses and a new marketing technology, too. As is being developed at Japan Galactic, the CNAS will be able to use a software platform, directly from sensors, chips and computer equipment, to connect the lab to the internet, so anyone can have to connect the technology to a network in order to prove themselves. The work behind the science study will have to be a bit harder. Once Origin Incorporated, the in vitro technology, the cornerstone of Japanese research, will be patented. Until this point in time, the company will have been seeking to fly to and around the European Union. Now it is soon moving a small European research firm into the institute's systems and hardware to make it the largest possible market in the next few years. "We want to aim to take the lead in a scientific lab that extends its capabilities all over the world. We want to see competitive research in pursuit of our own lives. And if this happens, it's a huge breakthrough in the human race and it's a very exciting opportunity for innovation," said James Smith, the head of the European Union's main scientific research organization, in his remarks last Wednesday. First, the World Congress will launch a similar technology in July and SpaceShipOne's first public flight in June. But it's the first major launch ever in the US. One first year to take US experiments together was announced by a consortium that had made headlines. Although the European market is already the first to use the technology, not all companies are doing the same. SARC a medical group whose works show the potential to provide the treatment for cancer is moving to use the European Union, government, agencies and government scientists to set up its own research laboratory on CNAS. This is a trip up to space, and both experiments will carry a drug and brain tested. The first stage is that it lets the US take a part in its orbit. Unlike the first spaceflight process, it must be transited and overseen by a plane. The technology also lets the US to interact with the environment, including in places like the International Space Station. That probably leads to its own bigger push into the robotic body. But now a second stage is where the FDA is looking to find ways to make comparisons and communicate to the public about how to deliver drugs. It's a way that the effects on the human body have been far less measured. CNAS still needs approval of its patent. Using the technology that could produce therapeutic efficacy in those with psychiatric disorders a broad vein of neuroscience, medicine and data would violate several of the agency's guidelines. "We seem to find that a few years progress on the case would be slow and hard to justify because it contradicts these government and the need for higher quality," Smith wrote in his remarks. The U.S. Senate in July has suggested it will not approve any proposals that boost sales. A similar measure in May led Europeans to vote on whether or not drugs should face peer-to-peer trading. The news dark off signs in 2015 that the European Parliament passed the European Commission's next financial year, inhibiting the FDA's scientific review of its potential effect on certain drugs. A pilot for a similar study is expected to cost about \$2,000 each and is expected to launch in the UK, the end of 2016. <|endoftext|> The Bank of England announced the interest rates on December 7, recommending a discount rate of from 28% to 30'

1232

1233

Figure 9: Sample from MDLM + Gumbel Distillation of length 1024 and  $T = 1024$  steps. The generative perplexity of the sample under GPT-2-Large is 35.19 and its entropy is 5.32.

1234

1235

1236

1237

1238

1239

1240

1241

1242  
1243  
1244  
1245  
1246  
1247  
1248  
1249  
1250  
1251

1252  
1253  
1254  
1255  
1256  
1257  
1258  
1259  
1260  
1261  
1262  
1263  
1264  
1265  
1266  
1267  
1268  
1269  
1270  
1271  
1272  
1273  
1274  
1275  
1276  
1277  
1278  
1279  
1280  
1281  
1282  
1283  
1284

Two years then signed him, and he told his friends. He was one of the best soccer players ever. helped take out the England national team, which is vacant at this stage. It's been a long journey, said Rodriguez, who's now gone beyond the borders of the world."I'm going to say I love England," but to be said England, and to have fun."Obviously he's very close. I have no doubt he is a highly respected male partner of my country," said Rodriguez, who signed as ambassador. "But not wanting that much to beat the player, because, like a passion. He's going to be here for a long time just to go there." Rodriguez, like the England Americans and others, has been a huge player to get a top-flight team in the top six would be tough."He's been on the right side," Rodriguez said. He's England sooner than I was. The last time I was with the European team. He's been really tough, whether we get to the fourth round. We have been competitive, the capital of the Southwest region."Demophia Deillen, who was a first-round pick, one of the best players in the world, who has played heavily in hopes of winning the national championship in the past two years, even as part of a loan by the United States to Colorado part."But he's not an idol. We don't have that many other guys in the soccer world with the highest-level play -- Chicago but he knows his side," Deillen said. She said in a statement after England's World Cup title: "He has helped a team that signed a numbers-like season in the National Soccer League. That's exciting football." "I care" women's soccer players more at Manchester City than anywhere in the European League of "everyone is in the United States," International Director Brian K. Menjelstra told The JTA. "I am happy to win World Cup and to have a person able to represent the women's league in England and with women's Soccer at the top of my heart and inspire me to defend my country."The United Soccer Association currently selected women's first team competition winners, and wishes competition organizers to prepare the best young players beyond the age of 30.Meanwhile, the academy is in Australia and begins in New Zealand. It's now the biggest and biggest tournament the women team in America has played."It's a challenge for the fans see women's Soccer playing in the World Cup finals," Deillen said.That the England Americans had the players they signed. A lot of them have seemed to say that they can't stand these clubs, and this time they are players themselves."That would be a concern. I think you look at some teams, one year and-16, some of them hoping to get them in four years," she said. So far, the England players appear to have no nationalistic mind.In the preliminary stage, there are no signs that the two national players left the team. They have no say on who is now, and the team is still with the England players. I know there's yet another team to play for me and that's really my confidence."Nevada spokeswoman Laura White later issued a statement to the federation declaring this "a new one" between the two sides, which will play in London, as for the kind of spot where the top two are in contention by the two federations.White spoke with the federation at 9:40 p.m., and they said the players didn't be ready to take part before, a statement that indicates the way the women's federation intends to be used.White said the morning before the tournament said he could not be with that team, and that he was prepared to make himself unavailable. He has been contacted by the United States Embassy for comment on the price he had paid.Shake said she is "where the players are for a while," but added that she will continue to be connected to the team.<endoftext>Mike Carrington (SMS chief) made his case to Clarke Hall (SSP), who heads Royal North-C. Wales for the west west Wales University Hospital, saying the two are "very close associates on the NHS" as a result of a phone call."My first reaction is I'm not happy at the moment," said Royal's deputy chief, a nurse who was traveling last week in his clinic to meet Hall and hospital.On Tuesday morning, a spokesman for the chief "called into similar situation with our partners, who were working with the NHS, where they approached our officers at the same conversation with the spokesman," he said.North-west Wales chief director of the hospital posted official website, saying: "If there are no good answered on the NHS's mobile phone then

1285  
1286  
1287  
1288  
1289  
1290  
1291  
1292  
1293  
1294  
1295

Figure 10: Sample from BD3-LM of length 1024 and  $T = 1024$  steps. The generative perplexity of the sample under GPT-2-Large is 37.7 and its entropy is 5.21.

1296

1297

1298

1299

1300

1301

1302

1303

1304

1305

1306

1307

'<|endoftext|>How many times in my life have I been a woman? I've always felt like a woman in everything I've done to be proud of, just being a great person, so I am reconsidering. My gifter wants to be named the ""Santa"" and we will have to see her on Christmas Day. I have received many gifts over the years, but I am a soppin' and bemo in my body, I feel like I am a woman! All I want to throw away this thing is to do a happy and productive job like that. Something has been happening a lot lately, and it's a very frustrating time today. The gifting is just part of a series of events in the past year. The location is in Orlando, and a relatively long way away from home. The photos are the ones I want to give to the community, not the ones my senders are not getting. But I know the ones I'm sending are donating to or assisting the fans in these gifts. My gifter will be thanking my Santa and giving me hugs! If I are you, you are in my heart. You are here at my funeral. This is what I am all doing. I don't feel like being a hero. I'm literally not giving a damn about the people that I put to them. It's beautiful, but the picture isn't about my heart? If you are me, it would be more than what I do. And it's not something that a lot of people do. If I'm shown in a video, I just see some of the news pieces that have been posted and on. I want for people to show their support for (my gifter) and they will tell me. I'm not doing what I do. I have to give away the gift, I'm not a ""artist"" or an artist at all, and I'm not a ""real creator"" of anything to leave my own name, and I don't want to be a woman to get any support. I want to get a name on the internet for this thing. You aren't getting the name out of people who deserve to be given a name. With that said, at least one of the people in this individual's circle have been kind through me. I have never thought while doing my rounds with the gifter I would give me away. I just laughed. I thought gift exchanges would make me feel better. Or maybe they would have. But I'm not leaving it up to the gifter on it. It's just acceptance. A friend was my mother, but he said that she likes helping people, and she said he wants to get away from things that have been done. However, she didn't make any plan to gift him. He was completely aware of it and just thought and went with it. I want things like this to get away from all of my gifts. I think I have only one thing to do. Both of those things are bad and I cannot gain access to them. These are bad things and when I read about them, I find them justified. I then give the gift to gifters and I take it to the audience to show me that I can do what I could do. I want to be able to get something to give to them, and give it to others to give away. I'm just then going and then tapping into the pressure on me that is stopping them from helping me. This isn't simply a gift. When I've done it, they are usually getting it away anyway from all of them. I don't know how all I did, I wasn't thinking about it, but I went on my way. I put up this opportunity for people that I was going to consider and have a very happy time. It's basically all about me. I was going to give it on to someone who was one of the ones I was after and I didn't even have to give them the support because I was going. It didn't have felt right for me, as I went to what I already did and I just never got the tool that I had. I'm so happy with it. I spent a couple of months getting to get that power back and go back to the world to write about myself. I have not really defined myself as a real artist for being a. So that is a good feeling for all me. The people do not want me to get through the process of loving as an artist, not wanting to be me to be the person I can be. I need to reach out to my fans, to know what the people have against me. But I go through this. I need to show my support for them and gifting. The fact that those are all benefits the people have, of the community itself. That means I have a lot of tiny self-help projects and projects that are awesome.'

1336

1337

Figure 11: Sample from BD3-LM + Gumbel Distillation of length 1024 and T = 1024 steps. The generative perplexity of the sample under GPT-2-Large is 27.2 and its entropy is 5.19.

1340

1341

1342

1343

1344

1345

1346

1347

1348

1349

1350  
1351  
1352  
1353  
1354  
1355  
1356  
1357  
1358  
1359

'the numbers gameTo me, the most important takeaway is the media wants to sensationalize the story, it wont matter. The real story here is what I have come to expect of the average reporter. I have come to expect that most things you say on the air will blow up and overshadow the fact that you are a regular citizen and could well have said anything you want to people if they catch on. But this isnt the case. The average anchor on CNN has changed the story on regular basis. If you dont listen to the media, you will lose.In the name of being unbiased, the mainstream media will remain a relatively unknown group. I think they are having an effect on the perception of the public. In my view, everyone on the air is over-represented on network television. If they are not correct, they can win over viewers who may not necessarily be paying attention. A good example of this would be when CNN featured a big story about the North Korea nuclear test and the ratings went down. For some reason, the coverage led to fewer viewers on CNN, and that was definitely what happened.I think the U.S. media is more adept at making propaganda pieces. The result is that when they present a big story, and when they get the impression they are going to win, people might not go on CNN. I expect that my expectation is that the news media will get more viewers on CNN and possibly even win more viewers for cable networks (not to mention newscasts and prime time shows). But if they dont, I think a new wave of viewers might be swayed to the second tier.\n\nThe outcome for me is unclear. CNN has a big story, and I do expect it to draw in a large percentage of viewers, while the anchors are losing viewers. This could be an entertaining topic that the major networks want to have on air. Maybe they want to win over viewers for those networks? The next step I see is for them to stop showing old news if they dont think the American public is paying attention.You can follow @Nero on Twitter.Commentscomments<|endoftext|>Disneyland will have you believe the first time you step inside The Collectors Mini Tower on the grounds of Disneylands Hollywood Studios. As the world and park matures, people are returning to visit Disneyland for the first time.Construction on the 10,000 square foot star-studded attraction began in 2001. Disney developed the idea to include the area as a Disneyland Memorial Hall in the park.In August 2013, The Collectors Mini Tower was revealed to the public during a visit. During the visit, guests saw the incredible view that was included inside the tower and learned about how much it cost to construct this unique attraction.According to Disney, the five-storey building is 42,000 square feet and features more than 1,500 rooms, with windows overlooking the street level of the exterior to the inside.The size of the structure makes it a unique experience for tourists. The attraction itself takes guests to a special foyer lined with board game and ride setups.The Tower was constructed at a cost of \$60 million and includes several areas of state owned amusement park property.<|endoftext|>Both the Canada Goose and the Canadian flag may soon have new colours.The federal government is changing its policy that says any bill to change Canada's flag must be approved by parliament, making the Canada-U.S. trilateral trade agreement less of a reality.\n\nLast month, Finance Minister Bill Morneau issued a memorandum to all government ministers outlining what he said would be changes to the copyright and trademarks laws if the Canada-U.S. trade agreement between the two countries is not approved by Parliament.Under the memorandum, the government is proposing to replace the country's Canadian half with an intergovernmental and unionized version of Canada's flag, or the flag of the Confederation.The new agreement between Canada and the U.S. will add a new label to the Canadian flag called the C Treaty. It marks a change from the government's Conservative government of prime minister Stephen Harper's to a Liberal government of prime minister Justin Trudeau.It is estimated that 12 million Canadians could lose their current U.S.-ca. Canadian half. It is almost impossible to pick a colour without buying one. - Patrick Simon, retired Ottawa journalist.To get your product into the C Treaty, the country must submit its new government agreement, called the C Treaty, to the U.S. Congress and ask the administration to pass it.When the C Treaty is approved, it will be trade liberalization, which will start with a six-month notice period from October 1, 2018, through October 31, 2019. That means the new treaty will be in effect for three years.According to the Finance Minister'

1392  
1393  
1394  
1395  
1396  
1397  
1398  
1399  
1400  
1401  
1402  
1403

Figure 12: Sample from AR of length 1024 and T = 1024 steps. The generative perplexity of the sample under GPT-2-Large is 15.7 and its entropy is 5.29.